Title: High Density Lipoproteinspotentiate α-1 antitrypsin therapy in elastase-induced pulmonary emphysema

Authors: Juan-Antonio Moreno[1,2], Almudena Ortega-Gomez[1], Alfonso Rubio-Navarro[2], Liliane Louedec[1], Benoit Ho-Tin-Noé[1], Giuseppina Caligiuri[1], Antonino Nicoletti[1,3], Angelique Levoye[1,4] , Laurent Plantier3[,5,6] and Olivier Meilhac[1,3,7]*

Affiliations:

[1]Institut National de la Santé et de la Recherche Médicale (INSERM) Unité Mixte de Recherche (UMR)1148, DHU FIRE (Département Hospitalo-Universitaire Fibrosis, Inflammation, REmodeling in cardiovascular, respiratory and renal diseases), Paris, France
[2]Vascular Research Laboratory, Instituto de Investigación Sanitaria-Fundación Jiménez Díaz, Madrid, Spain

[3]Universite Paris Diderot, Sorbonne Paris Cité, Paris, France
[4]Universite Paris, Sorbonne Paris Cité, France

[5]INSERM UMR700, DHU FIRE, Paris, France
[6]Assisance Publique des Hôpitaux de Paris, Department of Physiology, Paris, France; and
[7]Centre Hospitalier Universitaire de La Réunion, Saint-Denis, France

*Address for correspondence: Olivier Meilhac. INSERM U698, CHU Bichat,46, rue Henri Huchard75877 Paris Cedex 18, France. Tel : 33-1-40-25-86-00, Fax : 33-1-40-25-86-02

Email : **olivier.meilhac@inserm.fr**

Running title: HDL- α-1 antitrypsin co-treatment in emphysema

Funding: This research was supported by ANR JCJC-1105 HDLomics, Fondation de France, Fondation Coeur et Artère and FIS (Programa Sara Borrell and Miguel Servet (CP10/00479)) and PI13/00802 to JAM.

ABSTRACT

Several studies report that high-density lipoproteins (HDLs) can carry α1-antitrypsin (AAT; an elastase inhibitor). We aimed to determine whether injection of exogenous HDL, enriched or not in AAT, may have protective effects against pulmonary emphysema. After tracheal instillation of saline or elastase, mice were randomly treated intravenously with saline, human plasma HDL (75 mg apolipoprotein A1/kg), HDL-AAT (75 mg apolipoprotein A1–3.75 mg AAT/kg), or AAT alone (3.75 mg/kg) at 2, 24, 48, and 72 hours. We have shown that HDL-AAT reached the lung and prevented the development of pulmonary emphysema by 59.3% at 3 weeks (alveoli mean chord length, 22.9 ± 2.8 μm versus 30.7 ± 4.5 μm; $P < 0.001$), whereas injection of HDL or AAT alone only showed a moderate, nonsignificant protective effect (28.2 ± 4.2 μm versus 30.7 ± 5 μm [$P = 0.23$] and 27.3 ± 5.66 μm versus 30.71 ± 4.96 μm [$P = 0.18$], respectively). Indeed, protection by HDL-AAT was significantly higher than that observed with HDL or AAT ($P = 0.006$ and $P = 0.048$, respectively). This protective effect was associated (at 6, 24, and 72 h) with: (1) a reduction in neutrophil and macrophage number in the bronchoalveolar lavage fluid; (2) decreased concentrations of IL-6, monocyte chemoattractant protein-1, and TNF-α in both bronchoalveolar lavage fluid and plasma; (3) a reduction in matrix metalloproteinase-2 and matrix metalloproteinase-9 activities; and (4) a reduction in the degradation of fibronectin, a marker of tissue damage. In addition, HDL-AAT reduced acute cigarette smoke–induced inflammatory response. Intravenous HDL-AAT treatment afforded a better protection against elastase-induced pulmonary emphysema than AAT alone, and may represent a significant development for the management of emphysema associated with AAT deficiency.

Key Words: HDL, alpha-1 antitrypsin, elastase, emphysema

Clinical Relevance

In addition to their antiatherogenic properties, high-density lipoproteins (HDLs) transport α1-antitrypsin (AAT) and display display antielastase activity. In our study, we show that the protective effects of HDL-AAT intravenous injection in an in vivo model of elastase-induced pulmonary emphysema were superior to those of AAT alone. Our results suggest that a treatment combining HDL and AAT may be more effective than the currently used AAT augmentation therapy

INTRODUCTION

Proteolytic degradation of the alveolar septa leading to airspace enlargement and development of pulmonary emphysema in patients exposed to cigarette smoke (CS) is thought to be the consequence of a protease/antiprotease imbalance. In particular, the increased incidence of emphysema in patients with α1-antitrypsin (AAT; product of the SERPINA1 gene) deficiency pointed at neutrophil elastase as the main effector of pulmonary proteolytic damage (1).

AAT is a 52-kD glycoprotein mainly produced by hepatocytes and then secreted into the bloodstream. Circulating AAT is the main inhibitor of neutrophil elastase, and diffuses into injured tissues, including the lungs, to prevent proteolytic damage (2). AAT deficiency leads to obstructive pulmonary diseases and liver dysfunction (3). Patients with emphysema associated with AAT deficiency are commonly treated weekly by intravenous infusions of highly purified human AAT. However, although intravenous AAT augmentation therapy has been demonstrated to be safe, high doses of AAT (60 mg/kg) need to be injected, as only about 2% reaches the epithelial lining fluid (2, 4), whereas therapeutic efficacy remains to be demonstrated (5). Our hypothesis is that a better vectorization of AAT may allow injection of lower doses of AAT and increase efficacy. A better bioavailability may widen the indication for treatment of individuals who have partial AAT deficiency (MZ heterozygotes), for example.

Beneficial effects of high-density lipoproteins (HDLs) in the context of cardiovascular disease are principally attributed to reverse transport of cholesterol, even though other antiatherogenic properties, such as antioxidant, anti-inflammatory, or antithrombotic effects, are well documented (6). Various studies using proteomic approaches have shown that many proteins other than its constitutive apolipoprotein A-I may be associated with HDL. We have recently described the presence of AAT in HDL, and have demonstrated that HDL inhibits elastase activity and prevents its associated effects, such as apoptosis (7). More importantly, in this study, we report that HDL can be enriched with AAT. HDL may thus represent a vector for proteins or peptides reported to be naturally associated with it, because of their affinity for HDL particles (8, 9). Acute administration of reconstituted HDL has been shown to normalize the endothelial dysfunction in patients with hypercholesterolemia (10, 11). In addition, HDL-based therapy has been shown to be beneficial in murine models of myocardial ischemia–reperfusion (12) and stroke (13).

In stroke, these protective effects were suggested to be associated with a protection of the blood brain barrier, in particular by limiting polymorphonuclear neutrophil (PMN) extravasation (13). PMNs, as a major source of elastase, play a key role in emphysema development. Interestingly, it was demonstrated in vivo that HDLs were able to inhibit cytokine-induced expression of endothelial adhesion molecules for leukocytes and then reduce PMN adhesion and transmigration (14). We thus hypothesized that injection of HDL or AAT-enriched HDL may decrease PMN recruitment into the lung and limit elastase-associated tissue damage.

In the present study, by using a mouse model of pulmonary emphysema induced by elastase, we show that treatment with AAT-enriched HDL limited the recruitment of PMNs and macrophages, and significantly reduced alveolar destruction, in comparison with treatment with AAT alone. Therefore, HDL enriched with AAT may represent a potential therapeutic option to limit pulmonary emphysema.

METHODS

Purification of HDL, enrichment with AAT and quality controls

HDLs (density [d] = 1.125–1.210 g/ml) were isolated from a pool of human plasma from healthy volunteers by ultracentrifugation as described previously (7). Briefly, after adjusting its density to 1.22 with potassium bromide (KBr), plasma was overlaid with KBr saline solution (d = 1.063 g/ml). Ultracentrifugation was performed at 100,000 × g for 20 hours at 10°C. The upper lipoprotein fraction containing low-density lipoproteins (LDLs) was eliminated and the density of the lower fraction containing HDLs was adjusted to 1.25 g/ml with KBr, and the resulting solution was overlaid with KBr saline solution (d = 1.21 g/ml). The HDL fraction was recovered at the top of the tube, and the KBr was eliminated using centrifugal filter devices (Vivaspin 5 kD molecular weight cut-off; Sartorius, Les Ulis, France). For HDL enrichment in AAT, HDLs (10 mg) were incubated for 16 hours with 10 mg of AAT in a total volume of 20 ml at 37°C under gentle shaking. HDLs were then reisolated by ultracentrifugation to eliminate unbound AAT. Western blot analysis against AAT and apolipoprotein A1 (ApoA1) were performed to verify HDL enrichment with AAT. Different amounts of AAT were also loaded to semiquantitatively assess the amount of AAT present in native and AAT-enriched HDL (see Figure 1A). In parallel, the antielastase activity of native and HDL-AAT was assayed using a chromogenic substrate for elastase (Figure 1B). Briefly, human neutrophil elastase (10 nM; Calbiochem, Darmstadt, Germany) was incubated with 1.5 mM of an elastase chromogenic substrate, MeO-Suc-Ala-Ala-Pro-Val-pNa (Calbiochem) in reaction buffer (5 mM Tris-HCl [pH 7.4], 100 mM NaCl, 0.01% Tween-20, 250 μl final volume). AAT (0.01–0.5 μg; Calbiochem), native and HDL-AAT (1–20 μg for dose–response experiments) were preincubated with elastase for 15 minutes at room temperature before he addition of the substrate. Substrate hydrolysis was monitored for 2 hours at 37°C at 405 nm.

Animal model of elastase-induced emphysema

We used a mouse model of emphysema induced by elastase, as previously described (15), characterized by an acute influx of PMNs into the lung, leading to the destruction of alveoli. Studies were conducted in 8 week-old C57BL/6 male mice (Janvier, Le Genest Saint-Isle, France), in compliance with Institut National de la Santé et de la Recherche Médicale guidelines regarding the fair treatment of animals, under a

license from the French administration to conduct animal research, as described in the protocol. Mice were anesthetized with ketamine/xylazine and then received a tracheal instillation of 50 μl of saline (sham group) or 5 U of porcine pancreatic elastase (Elastin Products, Owensville, MO) in 50 μl of saline into the surgically exposed trachea. Elastase-treated mice were then divided into four groups: injected with saline; HDL (75 mg/kg body weight); HDL enriched in AAT (75 mg ApoA1–3.75 mg AAT /kg); or the same amount of AAT alone (3.75 mg/kg) (Figure 1B).

In a first set of experiments, mice were injected intravenously 2 hours after elastase instillation and then every 24 hours for the first 3 days. After 28 days, mice (n = 10 per group) were anesthetized with ketamine/xylazine and their lungs were removed for morphometric analysis of alveolar destruction (see text below). In a second set of experiments, mice were anesthetized in a similar manner, blood was sampled from the vena cava on EDTA, and a bronchoalveolar lavage (BAL) was performed for further analysis at 6, 24, 48, and 72 hours after elastase instillation (n = 8 per group). In a third set of experiments, mice (n = 4 per group) were imaged 6 hours after elastase instillation and 4 hours after injection with 1,1′-Dioctadecyl-3,3,3′,3′-tetramethylindodicarbocyanine-5,5′-disulfonic acid (DilC18)-labeled HDL, DilC18-labeled HDL-AAT, or saline (see text below).

Acute model of cigarette smoke (CS) exposure

CS exposure was performed in a single exposure using smoke from three consecutive (with 5-min breaks in between) standard research nonfiltered cigarettes (2R1 [11.7 mg total particulate matter per cubic meter of air, 9.7 mg tar, and 0.85 mg nicotine per cigarette]; University of Kentucky, Lexington, KY). Mainstream CS was generated by an exposure system in which combustion of the cigarette was drawn into the mouse chambers via a peristaltic pump (KD Scientific, Inc., Holliston, MA). Research cigarettes were smoked according to the Federal Trade Commission protocol (1 puff/min of 2-s duration and 35 ml volume), with fresh air being pumped in for the remaining time. At 1 hour before CS exposure, mice were injected intravenously with saline, HDL (75 mg/kg body weight), HDL enriched in AAT (75 mg ApoA1–3.75 mg AAT /kg), or the same amount of AAT alone (3.75 mg/kg). Non–smoke-exposed mice were administered filtered air in an identical chamber according to the protocol described for CS exposure.

At 72 hours after CS exposure, we determined inflammatory response in BAL fluid (BALF) and inflammatory chemokine expression in lung tissues homogenates.

Morphological analysis

The lungs were fixed with 2.5% glutaraldehyde at a transpleural pressure of 25 cm H2O for 3 hours and then stored in 4% paraformaldehyde (Sigma-Aldrich, L'Isle d'Abeau, France). Great-axis sagittal sections (5 μm) of the left lung were cut in a systematic fashion, and were stained with hematoxylin and eosin. Five black-and-white digital photomicrographs were acquired from the cranial, medial, and caudal regions of each slide at ×100 magnification, excluding areas where large bronchi or vessels predominated, resulting in a total of 15 images per lung. Emphysema was then quantified by measurement of the mean chord length of alveoli with Analysis software (Soft Imaging System, Münster, Germany) at a 5-μm interval. This automated analysis was made vertically and horizontally on each photomicrograph. The analysis was performed in duplicate by two blinded observers (J.-A.M. and L.P.), resulting in a total of roughly 900,000–1,500,000 measurements per slide. The mean chord length of alveoli was obtained by averaging those measurements.

Bronchoalveolar lavage fluid

The lungs were lavaged with 2 ml of saline, and the resulting BALF was centrifuged at 300 × g for 15 minutes. The supernatant was stored at −20°C until analysis, and cells were washed three times and then analyzed on an LSRII cytometer (BD Biosciences, Le Pont de Claix, France). Phycoerythrin Rat Anti-Mouse Ly-6G (BD Biosciences) and FITC rat anti-mouse F4/80 (eBioscience, Paris, France) antibodies were used to detect neutrophils and monocyte/macrophages in BALF, respectively. The LIVE⁄DEAD Fixable Dead Cell Stain Kit (Invitrogen, Carlsbad, CA) was used to exclude dead cells from the analysis. Data were acquired and analyzed using FACSDiVaTM Software Version 6.13 (BD Biosciences).

Zymography

For gelatin zymography, 5 μl (6-h time point) or 20 μl (other time points) of BALF were electrophoresed on 10% SDS–polyacrylamide gels containing 1 mg/ml bovine gelatin (Sigma-Aldrich). Non–matrix metalloproteinase (MMP) gelatinolytic activity, in particular that of elastase, could be evidenced by addition of 2.5 mg/ml fucoidan (Sigma-Aldrich) to the resolving gel. SDS was removed from the gels by incubation in 100 ml

2.5% Triton X-100 (Sigma) twice for 1 hour under gentle shaking. The gels were then incubated for 2 days at 37°C in 50 mM Tris HCl containing 5 mM CaCl2, 1 μM ZnCl2, and 150 μM NaN3 (pH 7.5). MMP gelatinase (2, 9) and neutrophil elastase activities were assessed by quantifying the bands of proteolysis after Coomassie blue staining.

Soluble marker detection

Cytometric Bead Array Mouse Inflammation Kit (Becton Dickinson, BD Biosciences/Pharmingen, San Diego, CA) was used to quantify plasma and BALF levels of IL-6, monocyte chemoattractant protein (MCP)-1, TNF-α, IL-10, IFN-γ, and IL-12p70. Flow cytometry analysis was performed using a FACSCalibur flow cytometer (BD Biosciences). Data were acquired and analyzed using BD CBA Software, following the manufacturer's instructions. The sensitivities of the cytometric bead array assays for IL-6, MCP-1, and TNF-α, were 5.0, 52.7, and 7.3 pg/ml, respectively.

Immunohistological analysis

AAT and apoA1 were detected by immunohistofluorescence in frozen lung sections using a goat anti-AAT antibody diluted 1:50 (ab7635; Abcam, Paris, France) and a rabbit anti-apoA1 antibody diluted 1:100 (178,422; Calbiochem) applied for 1 hour at room temperature. Secondary anti-goat and anti-rabbit antibodies (respectively conjugated to Alexa 555 and 488; Invitrogen) were then added and incubated for 1 hour at room temperature. Anti-neutrophil antibody (rabbit anti-Ly6B2 antibody diluted 1:100; Serotec, Colmar, France) was applied overnight at 4°C. Secondary biotinylated anti-rabbit antibody was then added and incubated for 1 hour at room temperature. Negative controls using the corresponding irrelevant IgG were included to check for nonspecific staining. Then an avidin–biotin peroxidase complex (Vectastain ABC kit; Vector Laboratories, Burlingame, CA) was added for 30 minutes. Sections were stained with 3-amino-9-ethyl carbazol (DAKO, Glostrup, Denmark), and counterstained with hematoxylin.

Western Blot

Lungs were homogenized in lysis buffer (50 mM TrisHCl, 150 mM NaCl, 2 mM EDTA, 2 mM EGTA, 0.2% Triton X-100, 0.3% NP-40, 0.1 mM PMSF, and 1 μg/ml pepstatin A) and then separated by 10% SDS-PAGE under reducing conditions. After electrophoresis, samples were transferred to polyvinylidene difluoride membranes (Millipore, Bedford,

MA), blocked with 5% skimmed milk in PBS/0.5% vol/vol Tween 20 for 1 hour, washed with PBS/Tween, and incubated with goat anti-AAT antibody, diluted 1:1,000 (ab7635), and a rabbit anti-apoA1 antibody, diluted 1:1000 (178,422; Calbiochem), applied for 1 hour overnight. Antibodies were diluted in 5% milk PBS/Tween. Membranes were washed with PBS/Tween and incubated with appropriate horseradish peroxidase–conjugated secondary antibodies (1:2,000; Amersham, Aylesbury, UK). After washing with PBS/Tween, the fixed horseradish peroxidase antibodies were evidenced by the chemiluminescence method (ECL; Amersham). Membranes were then probed with a mouse anti–glyceraldehyde 3-phosphate dehydrogenase antibody (1:2,000; Millipore) to verify equal loading.

HDL Labeling with Carbocyanines

HDLs were incubated overnight at 37°C under gentle shaking with 10 μg/ml DiIC18 carbocyanines (Invitrogen) and then separated by ultracentrifugation as described previously here. Labeled HDLs (10 mg/kg) were administered intravenously and mice were killed from 2 to 48 hours after injection. Lungs were embedded in optimal cutting temperature medium and immediately frozen in liquid nitrogen. Lung sections (5 μm) were prepared with the use of a cryotome. Immunostaining was performed for AAT or ApoA1 as described previously here, and nuclei were stained with 4′,6-diamidino-2-phenylindole (DAPI; 0.5 μg/ml for 10 min), and the sections observed under an epifluorescence microscope.

Affinity of HDL and HDL-AAT for Elastase

Human neutrophil elastase was distributed in a 96-well microplate (Greiner Bio-One, Les Ulis, France) to a final concentration of 100 nM in antigen coating buffer (0.05 M Na_2CO_3, 0.05 M $NaHCO_3$, pH 9.5) and incubated for 2 hours at room temperature. The coating solution was removed and nonspecific sites were blocked by adding 200 μl of blocking buffer (PBS–3% BSA). The plate was then incubated for 2 hours at 37°C in the presence of increasing concentrations of DilC18-HDL or DilC18-HDL-AAT. Fluorescence was measured using Infinite M200 plate reader (Tecan, Durham, NC). The mean fluorescence of baseline controls (wells with no DilC18-HDL or DilC18-HDL-AAT) was subtracted from the total fluorescence to determine the net fluorescence for each well. Results were analyzed by PRISM (GraphPad Software Inc., San Diego, CA) and are expressed as means (± SEM).

In Vivo and Ex Vivo Imaging of Elastase-Damaged Lung

Mice were imaged 6 hours after elastase instillation and 4 hours after injection with DilC18-HDL, DilC18-HDL-AAT, or saline using the IVIS-Lumina Imaging System (Caliper Life Sciences Inc., Hopkinton, MA). Grayscale-reflected images and fluorescence images were superimposed and analyzed using Living Image 3.1 software (Xenogen Corp., Alameda, CA). For ex vivo imaging of lungs, mice were killed and then their perfused lung blocks were removed and rinsed with cold PBS. Images were generated using the IVIS-Lumina Imaging System to examine fluorescence signal from DilC18-labeled HDL.

RNA Extraction and Real-Time PCR

Total RNA from lung of mice instilled either with saline or elastase was obtained by the Trizol method (Invitrogen) and reverse transcribed with High Capacity cDNA Archive Kit and real-time PCR was performed on an ABI Prism 7,500 PCR system (Applied Biosystems, Foster City, CA) using the ΔCt method. Expression levels are given as ratios to glyceraldehyde 3-phosphate dehydrogenase. Predeveloped primer and probe assays were obtained for murine, MCP-1, IL-6, TNF-α, scavenger receptor class B member 1 (SRB-1), and ATP-binding cassette transporter 1 (ABCA1; Applied Biosystems).

Statistical Analysis

Data are expressed as means (± SD) and were analyzed with Statview 5.0 software (SAS Institute, Cary, NC). Data comparisons between experimental groups at each time point were analyzed with the Kruskall-Wallis test and the Mann-Whitney U-test. P values less than 0.05 were considered significant.

RESULTS

HDL enrichment with AAT

HDL particles were enriched with AAT, as described in the Materials and Methods section, before reisolation by ultracentrifugation. The yield of HDL enrichment was evaluated semiquantitatively by anti-AAT Western blot (Figure 1A) and more precisely by determination of HDL antielastase capacity using a chromogenic substrate (Figure 1B). Both techniques evaluated the enrichment of AAT at fivefold relative to native HDL (10–50 μg AAT/mg apoA1). Because HDLs were injected at 75 mg/kg, the same amount of free AAT was then injected in mice (3.75 mg/kg, AAT-alone group) to assess the potential benefit of AAT vectorization by HDL (HDL-AAT group). The study flow diagram is presented in Figure 1B. Saline, HDL, HDL-AAT, or AAT were injected 2 hours after the initial pancreatic elastase intratracheal instillation, which was rapidly eliminated by the mouse (16). The different injections were therefore tested for their ability to inhibit deleterious effects of neutrophil infiltration and associated elastase release. Because human AAT was used for enrichment of HDL, its ability to inhibit mouse elastase was evaluated in vitro. In Figure E1 in the online supplement, AAT is shown to inhibit mouse neutrophil elastase in a dose-dependent manner.

HDL-AAT treatment reduces elastase-induced emphysema development

Intratracheal instillation of elastase induced pulmonary emphysema, as shown in Figure 2. Mice instilled with elastase (group 2) had diffuse emphysema lesions, and their mean alveolar chord length was markedly increased compared with that of mice instilled with saline (group 1). Mice injected with HDL-AAT after elastase instillation showed only minimal and focal emphysematous changes, with a 59.33% reduction in the development of emphysema (22.9 ± 2.8 μm versus 30.7 ± 4.5 μm, $P < 0.001$), as compared with control animals, whereas injection of HDL or AAT alone had no effect (28.2 ± 4.2 μm versus 30.7 ± 5 μm [$P = 0.23$] and 27.3 ± 5.66 versus 30.71 ± 4.96 μm [$P = 0.18$], respectively). Mice treated with HDL-AAT were significantly protected against elastase-induced emphysema in comparison with mice treated with either HDL or AAT ($P = 0.006$ and $P = 0.048$, respectively). These beneficial effects were not due to an additive effect of HDL and AAT on emphysema development, but a potentiation of their beneficial properties. Thus, no significant reduction in mean alveolar chord length was observed in mice injected with HDL or AAT both alone or in combination (HDL/AAT); however,

administration of HDL enriched in AAT (HDL-AAT) showed minimal emphysema changes (Figure E2). No significant differences in mean chord length where observed when elastase-instilled mice were injected with LDL, confirming the specificity of the HDL response (see Figure E2).

Exogenous HDL accumulate in the lung after elastase-induced emphysema and improve AAT delivery

To test the bioavailability of HDL to the lungs, HDLs were labeled with carbocyanines and then injected intravenously in sham- or elastase-instilled mice (after 2 h, at 10 mg/kg). HDL reached the lungs and could be detected from 6 hours after injection (Figures 3A and E3). HDL bioavailability was increased in inflamed tissue, as observed in emphysematous mice, both in vivo and ex vivo in isolated lungs. We then incubated labeled HDL and HDL-AAT on lung cryosections from mice instilled with either elastase or saline. A higher presence of labeled HDL or HDL-AAT was observed in mice instilled with elastase as compared with sham mice (Figure 3B). This effect was more evident for HDL-AAT than for HDL alone, suggesting that AAT transported by HDL may be responsible for HDL-AAT accumulation in the lung. AAT associated with HDL could be taken up via HDL receptors, such as SRB-1 and ABCA1, and may therefore mediate HDL and HDL-AAT uptake. However, mRNA expression of these receptors only showed a trend toward an increased expression after elastase instillation, which did not reach statistical significance (Figure E4). Because AAT may interact with elastase released by infiltrating neutrophils, we performed additional experiments to determine whether HDLs can bind to emphysematous lungs via AAT–elastase interaction. We confirmed an increased interaction between elastase and HDL-AAT relative to nonenriched HDL (Figure 3C) that could allow increased accumulation of HDL-AAT via the abundant release of elastase by infiltrating neutrophils in mice with emphysema (Figure 3C). Finally, we tested the ability of HDL to vectorize AAT into the lung. Mice instilled with elastase and injected with HDL or HDL-AAT showed an enhanced accumulation of ApoA1/AAT in the lung, as determined by Western blot and immunofluorescence (Figures 4A and 4B; see Figure E5). More importantly, injection of HDL-AAT led to increased AAT accumulation in the lung of emphysematous mice relative to injection with nonenriched HDL and AAT alone, confirming our previous observations (Figure 4). A colocalization was observed between apoA1 and AAT immunostaining, indicating that AAT remained associated with the HDL particles until their uptake by lung cells (Figure

4C). Overall, our data suggest that enrichment of HDL with AAT supplies some sort of directionality toward sites containing free elastase, which could increase its beneficial effects.

HDL-AAT prevent elastase-induced increase in inflammatory cells in BALF

The inflammatory cell composition of the BALF varied with time after elastase instillation. Although few neutrophils could be observed in BALF of naive mice, they constituted the major fraction of cells in BALF 6 hours after elastase instillation (Figure 5A). HDL treatment reduced the elastase-induced increase in neutrophils in BALF. The neutrophil count in BALF of mice treated with HDL alone was reduced by 65% versus 77% in the HDL-AAT group at 6 hours ($P < 0.05$), and by 85% in the HDL-AAT group at Day 3 ($P < 0.05$) relative to untreated emphysematous mice. Significant differences were also observed between groups injected separately with HDL and AAT as compared with the HDL-AAT group at 72 hours. The same results were obtained by immunohistochemistry for detection of neutrophils in the lungs of mice treated with HDL-AAT 6 hours after instillation of elastase (Figure 5B). Macrophage count was increased in the BALF of elastase-treated mice from the sixth hour to Day 3 (Figure 5C), peaking at Day 3 (10-fold increase compared with saline group; $P < 0.05$), whereas the neutrophil number decreased. HDL-AAT treatment completely inhibited the elastase-induced increase in alveolar macrophage number at all time points, whereas HDL- or AAT-injected alone only decreased macrophage numbers at 24 and 72 hours. A significant decrease in alveolar macrophages was also observed when comparing the HDL and AAT groups to the HDL-AAT group at 72 hours.

HDL-AAT reduce MCP-1, IL-6 and TNF-α in the elastase-injured lung

To determine potential mechanisms involved in the inhibition of inflammatory cell influx observed in HDL-treated mice, we measured the pulmonary concentrations of MCP-1, IL-6, and TNF-α, cytokines that may participate in the recruitment of monocytes/macrophages and neutrophils at the site of inflammation (15). A multiplexed assay was performed on plasma and BALF to quantitatively determine the levels of these inflammatory cytokines (Figure 6). MCP-1, IL-6, and TNF-α protein levels were increased in elastase-treated mice versus controls at 24 hours, and remained high at 72 hours in both plasma and BALF. HDL-AAT treatment completely prevented elastase-induced elevation in MCP-1, IL-6, and TNF-α at 24 and 72 hours. HDL treatment had no

effect on IL-6 and MCP-1 levels in either BALF or plasma, but decreased TNF-α plasma concentration at 24 hours. TNF-α (in BALF and plasma) and MCP-1 (in plasma) concentrations at 24 hours were lower in AAT-treated versus untreated elastase-instilled mice. IL-10, IFN-γ, and IL-12p70 were below the detection limit in both BALF and plasma. Overall, the association of AAT with HDL exhibited the most powerful anti-inflammatory effects.

HDL-AAT modulate elastolytic activity in BALF

We tested whether the protective effects of HDL treatment might be associated with a reduced neutrophil elastase activity. At 6 and 24 hours after elastase instillation, zymography showed the presence of a 25-kD band of lysis in BALF, corresponding to endogenous neutrophil elastase (Figure 7A). This band was not detected in the BALF of sham mice either at 6 or 24 hours. The intensity of the endogenous neutrophil elastase band was lower in HDL-AAT–treated mice (Figure 7B). Interestingly, this protective effect was much higher compared with the administration of the same amount of AAT alone. In agreement with the decline in neutrophil influx at 72 hours (Figure 5A), no elastase activity could be detected at this time.

Decreased matrix metalloproteinase-2 and -9 activity in BALF of HDL-AAT-treated mice

Macrophages and neutrophils secrete MMPs (17, 18). Because the development of elastase-induced emphysema has been previously linked to the increased expression and activity of MMPs in the lung (19, 20), we tested whether the protective effect of AAT-enriched HDL could modulate gelatinase activities in BALF. Gelatin zymography allowed detection of two bands of lysis, corresponding to MMP-2 (73 kD) and MMP-9 (97 kD), respectively (Figure 7A). MMP-9 activity was markedly increased in the BALF of mice from the elastase group compared with that of sham mice (at 6 and 24 h; Figure 7C). BALF MMP-9 activity in the HDL-AAT group was reduced relative to that of the elastase-treated group. Compared with the untreated group, MMP-2 activity was increased in the BALF of elastase-injured mice during the first 72 hours (Figures 7A and 7D). HDL-AAT treatment limited induction of MMP-2 activity in the BALF of elastase-instilled mice at Days 1 and 3 (Figure 7D). Therefore, the potent protective effect of HDL-AAT treatment was associated with the inhibition of MMP-2 and MMP-9 activities in BALF. Interestingly, both leukocyte elastase and MMP-9 activities were strongly

decreased at 72 hours after the onset of emphysema, correlating with the BALF neutrophil count. This suggests that neutrophils are the principal source of MMP-9 and elastase in our emphysema model.

HDL-AAT reduce degradation of alveolar fibronectin following elastase injury

To determine whether HDL-AAT treatment prevented the proteolytic degradation of the alveolar extracellular matrix, we evaluated the presence of fibronectin fragments in BALF. Elastase instillation was followed by a persistent increase in BALF fibronectin fragments, peaking at 24 hours (Figure 8). HDL-AAT treatment limited fibronectin fragment release at 24 and 72 hours, whereas AAT injection only partially prevented this degradation of fibronectin, reaching statistical significance only at Day 3.

HDL treatment decreased cigarette-induced pulmonary inflammation.

Finally, we determined whether HDL therapy would decrease acute inflammatory response in a model of CS exposure in mice (Figure E6). Our results show a significant increase in the percentage of neutrophils in BALF 72 hours after CS exposure; however, no significant macrophage accumulation in BALF was observed. HDL treatment reduced CS-induced increase in neutrophils, although significant differences were only observed in mice treated with HDL-AAT. No significant reduction in neutrophil numbers was observed after AAT injection. To determine the potential mechanisms involved in this decreased inflammatory cell influx observed in HDL-treated mice, we determined MCP-1, IL-6, and TNF-α mRNA expression in lung tissue homogenates of CS mice. MCP-1 and IL-6 lung expression was induced after CS exposure as compared with control mice; however, no significant differences were observed for TNF-α. HDL and HDL-AAT injections decreased MCP-1 expression significantly as compared with untreated CS mice. Administration of HDL particles or AAT in CS mice did not reduce IL-6 mRNA expression. Overall, our data suggest that HDL-AAT treatment may partially limits neutrophil recruitment and MCP-1 release; this may potentially reduce acute CS-induced inflammatory response.

DISCUSSION

In the present study, we have demonstrated that intravenous administration of HDL enriched with AAT effectively decreased elastase-induced pulmonary inflammation, reduced MMP-2/-9 and elastase activities, and subsequent alveolar destruction, whereas HDL isolated from human plasma (containing small amounts of AAT) or purified AAT alone only showed incomplete anti-inflammatory effects. The same protective anti-inflammatory effects were observed in an acute model of CS exposure. Our results suggest a vectorization of AAT by HDL to the injured lungs.

Numerous reports have demonstrated that the mouse model of emphysema induced by elastase reproduces the main pathophysiological mechanisms of pulmonary emphysema secondary to CS exposure and AAT deficiency in humans (21). This model is widely used in the lack of a genetic mouse model of human AAT deficiency, due to significant differences between human and mouse gene families (22). The elastase model is characterized by an important leukocyte extravasation preceding emphysematous changes (23). A marked increase in neutrophil infiltration could be evidenced by flow cytometric analysis of BALF at 6 hours after elastase instillation, whereas macrophages peaked at 72 hours. Interestingly, both HDL and HDL-AAT injection limited inflammatory cell infiltration, and, to a lesser extent, AAT. HDLs have been previously reported to inhibit leukocyte activation, adhesion, spreading, and migration in vivo in both mice and humans (24). These beneficial effects of HDL have been mainly described in vascular diseases, neurogenerative disorders, and cancer (6). Recently, important roles for HDL in lung biology have also been reported. For example, HDLs increase surfactant production by alveolar epithelium (25), and serve as the major source of the antioxidant vitamin E for alveolar epithelial cells (26). Furthermore, increased oxidative stress, inflammation, and fibrosis were described in the lungs of HDL-deficient ApoA1 mice (27).

To explore the mechanisms involved in the anti-inflammatory effect of HDL in our mouse model of emphysema, we determined the concentrations of three cytokines involved in the recruitment of neutrophils and monocytes in BALF and in plasma: MCP-1, IL-6, and TNF-α. Both BALF and plasma levels of these cytokines were increased after elastase instillation. TNF-α levels were increased at 24 hours after elastase instillation, whereas IL-6 and MCP-1 levels were higher at 72 hours. Interestingly, intravenous injections of

HDL, HDL-AAT, and AAT caused reduction in BALF and plasma levels of these cytokines, but only HDL-AAT administration consistently provided a statistically significant protection relative to the saline-injected group.

In addition to leukocyte invasion, an imbalance between proteolytic/elastolytic versus antiprotease activities in the lung may also play an essential role in the development of emphysema. MMPs and elastase are crucial effectors in the pathogenesis of emphysema, as reported in both humans (28, 29) and mice exposed to elastase (16). Increases in elastase, MMP-2, and MMP-9 activities were detected in the BALF of mice 6 and 24 hours after elastase instillation. These proteases are able to degrade extracellular matrix proteins of the alveoli, such as fibronectin, reflected by the increased levels of fibronectin fragments observed in the BALF of elastase-treated mice.

Proteolytic activities associated with induction of emphysema were partially reduced in the BALF of HDL-AAT–injected mice, suggesting an inhibition of the expression and/or release of gelatinases and elastase by the treatment. MMP-9 and elastase were detected in higher amounts at 6 and 24 hours after the initial injury, suggesting that they could be of neutrophilic origin. The inflamed lung tissue may also participate in protease production; it was recently reported that alveolar epithelial cells were able to produce and secrete MMPs (30), and that overexpression of TNF-α in the lung induced expression of MMP-2 and -9 (31). In agreement with our results, HDLs have been shown to inhibit the expression and activation of MMP-2 and -9 induced by oxidized LDL in smooth muscle cells (32) and macrophages (33). Moreover, infusion of plasma-derived and synthetic HDL prevented MMP-9 expression in rabbit aortic lesions (34), and attenuated ischemia–reperfusion–induced cardiac MMP-2 activation (35).

Since 1988, emphysema associated with AAT deficiency has commonly been treated with AAT augmentation therapy, which consists of regular intravenous infusions of purified human AAT at a weekly dose of 60 mg/kg (36). Such high doses of AAT need to be injected, because only about 2% reaches the epithelial lining fluid. This could explain why, in our study, injection of only 3.75 mg AAT/kg was not sufficient to prevent elastase-induced emphysema. Importantly, injection of the same amount of AAT combined with HDL led to increased AAT accumulation in the lung of emphysematous mice, and was able to limit lung injury. These results suggest that HDL could represent a

better means of delivering AAT, thus preventing emphysema with lower doses of AAT. The exact mechanism that would explain the increased bioavailabity of AAT when combined with HDL is not known. Our data show that AAT transported in HDL may interact with elastase released by infiltrating neutrophils in mice with emphysema, suggesting that enrichment of HDL with AAT supplies some sort of directionality toward sites containing free elastase, which could increase its beneficial effects. However, we cannot exclude the possibility that other potential mechanism may be involved in AAT bioavailability. AAT associated with HDL could be taken up via HDL receptors, such as SRB-1, which could increase significantly the intracellular concentration of AAT. Interestingly, both HDL receptors, SRB-I and ABCA1, are expressed by lung cells (26, 37), and may therefore mediate HDL/HDL-AAT uptake. However, mRNA expression of these receptors was unchanged after induction of emphysema in our study. On the other hand, it has been reported that endocytosis of AAT by the lung endothelium is mediated by clathrin, and may be an important determinant for protection against emphysema (38). The same group reported that AAT could prevent apoptosis of endothelial cells (39) via the intracellular inhibition of caspase 3 (40). The synergistic uptake of HDL-AAT by AAT acceptors and HDL-AAT binding to elastase released by infiltrating neutrophils may provide an explanation for the marked accumulation of HDL-AAT in our model. In addition to its antielastase property, AAT displays many protective properties, including antiapoptotic and immunomodulatory effects (41), and inhibition of MMP-9 (42), but was also shown to provide an important protection in a mouse model of myocardial ischemia–reperfusion (43). This suggests that AAT treatment could be considered in pathological conditions other than pulmonary emphysema (44). Because HDL particles also possess many pleiotropic effects (antioxidant, anti-inflammatory, antithrombotic, etc.), their combination with AAT may provide synergistic effects, in addition to an improved bioavailability in inflamed tissues.

HDL-based therapy has been shown to be effective in various acute experimental models, such as myocardial ischemia–reperfusion, hemorrhagic shock, or stroke (12–14). In this context, our study has some limitations. Indeed, in our model of emphysema induced by intratracheal elastase instillation, there is a single episode of acute lung injury resulting in alveolar destruction. In humans, injurious events are chronic, and the evolution of the pathology may take decades. This should be taken into account when evaluating the therapeutic implications of our results. Chronic treatment with HDL enriched by AAT

could be considered to limit the progression of emphysema in a population at risk, such as patients with AAT deficiency. It is also important to note that we used purified human HDL that contained all the associated—and potentially protective—proteins/other molecules (7). HDL is a carrier for sphingosine 1-phosphate (S1P), an antiapoptotic and anti-inflammatory molecule involved in maintenance of endothelial function (45). It has been reported that HDL induced cytoprotective effects via S1P in human endothelial cells by limiting apoptosis and by reducing the expression of adhesion molecules (46, 47). Furthermore, augmentation of the S1P signaling may protect from emphysema development via attenuation of airspace enlargement and apoptosis (48). In our study, different pools of HDL were used with similar results, suggesting that potential differences in protein or lipid composition between the different batches did not significantly affect the protective effect of HDL. For a potential therapeutic application, reconstituted HDL made of apoA1 and phosphatidylcholines could be used in combination with purified AAT. The cost effectiveness of this new augmentation therapy for AAT (49) should be estimated, as well as the feasibility of using reconstituted HDL enrichment with AAT.

The relation between HDL and pulmonary disease remains unclear. A number of studies have shown that HDL levels are increased in patients with emphysema and severe chronic obstructive pulmonary disease (COPD) (50, 51). Furthermore lung transplantation reduced HDL plasma levels in patients with COPD (52). On the other hand, lower plasma HDL concentrations were associated with lower lung forced expiratory volume in 1 second (53), and advanced COPD and emphysema (54). Several hypotheses may explain these discrepancies. First, patients with low HDL levels display an increased mortality, and may thus die by cardiovascular events before the development of advanced COPD; however, no studies have confirmed this hypothesis. Second, increased HDL levels may represent a response to proteolytic and oxidative insults that characterize emphysema. It is known that HDLs stimulate surfactant production by alveolar epithelial cells and growth of lung fibroblasts (25, 55). However, HDL is the major source of the antioxidant vitamin E for alveolar epithelium (26), and is a carrier for anti-inflammatory and antiapoptotic S1P, as previously reported (45–48). Furthermore, the lungs of HDL-deficient ApoA1 null mice showed increased fibrosis, oxidative stress, inflammation, and airway hyperresponsiveness (27). Thus, the relationship between circulating HDL levels and pulmonary outcomes deserves further investigation.

In conclusion, we found a beneficial effect of HDL-AAT infusion in an in vivo model of elastase-driven pulmonary emphysema, superior to that of AAT alone. HDL-based vectorization of AAT may increase efficacy of AAT augmentation therapy.

ACKNOWLEDGMENTS

The authors thank Drs. Jorge Boczkowksi, Laurent Boyer, and Sandra Perez Rial for fruitful discussions, Dr. Mary Osborne-Pellegrin for help in editing this manuscript, and Olivier Thibaudeau from the morphology platform of Institute Claude Bernard (ICB-Bichat) for histology.

REFERENCES

1. Eriksson S. Pulmonary emphysema and alpha1-antitrypsin deficiency.Acta Med Scand.1964.175:197-205

2. Hubbard RC, Crystal RG. Alpha-1-antitrypsin augmentation therapy for alpha-1-antitrypsin deficiency.Am J Med. 1988.84:52-62

3. Tuder RM, Janciauskiene SM, Petrache I. Lung disease associated with alpha1-antitrypsin deficiency. Proc Am Thorac Soc.2010.7:381-386

4. Kueppers F. The role of augmentation therapy in alpha-1 antitrypsin deficiency.Curr Med Res Opin.2011.27:579-588

5. Stoller JK, Aboussouan LS. A review of alpha1-antitrypsin deficiency.Am J RespirCrit Care Med.2012.185:246-259

6. Barter PJ, Nicholls S, Rye KA, Anantharamaiah GM, Navab M, Fogelman AM. Antiinflammatory properties of hdl. Circ Res.2004.95:764-772

7. Ortiz-Munoz G, Houard X, Martin-Ventura JL, Ishida BY, Loyau S, Rossignol P, Moreno JA, Kane JP, Chalkley RJ, Burlingame AL, Michel JB, Meilhac O. Hdlantielastase activity prevents smooth muscle cell anoikis, a potential new antiatherogenic property. FASEB J.2009.23:3129-3139

8. Karlsson H, Leanderson P, Tagesson C, Lindahl M. Lipoproteomics ii: Mapping of proteins in high-density lipoprotein using two-dimensional gel electrophoresis and mass spectrometry. Proteomics.2005.5:1431-1445

9. Vaisar T, Pennathur S, Green PS, Gharib SA, Hoofnagle AN, Cheung MC, Byun J, Vuletic S, Kassim S, Singh P, Chea H, Knopp RH, Brunzell J, Geary R, Chait A, Zhao XQ, Elkon K, Marcovina S, Ridker P, Oram JF, Heinecke JW. Shotgun proteomics implicates protease inhibition and complement activation in the antiinflammatory properties of hdl. J Clin Invest.2007.117:746-756

10. Bisoendial RJ, Hovingh GK, Levels JH, Lerch PG, Andresen I, Hayden MR, Kastelein JJ, Stroes ES. Restoration of endothelial function by increasing high-density lipoprotein in subjects with isolated low high-density lipoprotein.Circulation.2003.107:2944-2948

11. Spieker LE, Sudano I, Hurlimann D, Lerch PG, Lang MG, Binggeli C, Corti R, Ruschitzka F, Luscher TF, Noll G. High-density lipoprotein restores endothelial function in hypercholesterolemic men. Circulation.2002.105:1399-1402

12. Theilmeier G, Schmidt C, Herrmann J, Keul P, Schafers M, Herrgott I, Mersmann J, Larmann J, Hermann S, Stypmann J, Schober O, Hildebrand R, Schulz R, Heusch G,

Haude M, von Wnuck Lipinski K, Herzog C, Schmitz M, Erbel R, Chun J, Levkau B. High-density lipoproteins and their constituent, sphingosine-1-phosphate, directly protect the heart against ischemia/reperfusion injury in vivo via the s1p3 lysophospholipid receptor. Circulation.2006.114:1403-1409

13. Lapergue B, Moreno JA, Dang BQ, Coutard M, Delbosc S, Raphaeli G, Auge N, Klein I, Mazighi M, Michel JB, Amarenco P, Meilhac O. Protective effect of high-density lipoprotein-based therapy in a model of embolic stroke. Stroke.2010.41:1536-1542

14. Cockerill GW, McDonald MC, Mota-Filipe H, Cuzzocrea S, Miller NE, Thiemermann C. High density lipoproteins reduce organ injury and organ dysfunction in a rat model of hemorrhagic shock. FASEB J.2001.15:1941-1952

15. Plantier L, Marchand-Adam S, AnticoArciuch VG, Boyer L, De Coster C, Marchal J, Bachoual R, Mailleux A, Boczkowski J, Crestani B. Keratinocyte growth factor protects against elastase-induced pulmonary emphysema in mice. Am J Physiol Lung Cell MolPhysiol2007.293:L1230-1239

16. Starcher B, Peterson B. The kinetics of elastolysis: Elastin catabolism during experimentally induced fibrosis. Exp Lung Res.1999.25:407-424

17. Finlay GA, O'Driscoll LR, Russell KJ, D'Arcy EM, Masterson JB, FitzGerald MX, O'Connor CM. Matrix metalloproteinase expression and production by alveolar macrophages in emphysema. Am J RespirCrit Care Med.1997.156:240-247

18. Mackarel AJ, Cottell DC, Russell KJ, FitzGerald MX, O'Connor CM. Migration of neutrophils across human pulmonary endothelial cells is not blocked by matrix metalloproteinase or serine protease inhibitors Am J Respir Cell MolBiol.1999.20:1209-1219

19. Birrell MA, Wong S, Hele DJ, McCluskie K, Hardaker E, Belvisi MG. Steroid-resistant inflammation in a rat model of chronic obstructive pulmonary disease is associated with a lack of nuclear factor-kappab pathway activation. Am J RespirCrit Care Med.2005.172:74-84

20. Houghton AM, Quintero PA, Perkins DL, Kobayashi DK, Kelley DG, Marconcini LA, Mecham RP, Senior RM, Shapiro SD. Elastin fragments drive disease progression in a murine model of emphysema. J Clin Invest.2006.116:753-759

21. Kaplan PD, Kuhn C, Pierce JA. The induction of emphysema with elastase. I. The evolution of the lesion and the influence of serum. J Lab Clin Med.1973.82:349-356

22. Forsyth S, Horvath A, Coughlin P. A review and comparison of the murine alpha1-antitrypsin and alpha1-antichymotrypsin multigene clusters with the human clade a serpins. Genomics.2003.81:336-345
23. Lucey EC, Keane J, Kuang PP, Snider GL, Goldstein RH. Severity of elastase-induced emphysema is decreased in tumor necrosis factor-alpha and interleukin-1beta receptor-deficient mice. Lab Invest.2002.82:79-85
24. Murphy AJ, Woollard KJ, Suhartoyo A, Stirzaker RA, Shaw J, Sviridov D, Chin-Dusting JP. Neutrophil activation is attenuated by high-density lipoprotein and apolipoproteinA-I in in vitro and in vivo models of inflammation. ArteriosclerThrombVascBiol.2011.31:1333-1341
25. Pian MS, Dobbs LG. Lipoprotein-stimulated surfactant secretion in alveolar type II cells: Mediation by heterotrimeric g proteins. Am J Physiol.1997.273:L634-639
26. Kolleck I, Schlame M, Fechner H, Looman AC, Wissel H, Rustow B. Hdl is the major source of vitamin e for type ii pneumocytes. Free RadicBiol Med.1999.27:882-890
27. Wang W, Xu H, Shi Y, Nandedkar S, Zhang H, Gao H, Feroah T, Weihrauch D, Schulte ML, Jones DW, Jarzembowski J, Sorci-Thomas M, Pritchard KA, Jr. Genetic deletion of apolipoprotein a-i increases airway hyperresponsiveness, inflammation, and collagen deposition in the lung. J Lipid Res.2010.51:2560-2570
28. Ito I, Nagai S, Handa T, Muro S, Hirai T, Tsukino M, Mishima M. Matrix metalloproteinase-9 promoter polymorphism associated with upper lung dominant emphysema. Am J RespirCrit Care Med.2005.172:1378-1382
29. Taraseviciene-Stewart L, Voelkel NF. Molecular pathogenesis of emphysema. The J Clin Invest.2008.118:394-402
30. Pardo A, Ridge K, Uhal B, Sznajder JI, Selman M. Lung alveolar epithelial cells synthesize interstitial collagenase and gelatinases a and b in vitro. Int J Biochem Cell Biol.1997.29:901-910
31. Thomson EM, Williams A, Yauk CL, Vincent R. Overexpression of tumor necrosis factor-alpha in the lungs alters immune response, matrix remodeling, and repair and maintenance pathways. Am J Pathol.2012.180:1413-1430
32. Robbesyn F, Auge N, Vindis C, Cantero AV, Barbaras R, Negre-Salvayre A, Salvayre R. High-density lipoproteins prevent the oxidized low-density lipoprotein-induced epidermal [corrected] growth factor receptor activation and subsequent matrix metalloproteinase-2 upregulation. ArteriosclerThrombVascBiol.2005.25:1206-1212

33. Xu XP, Meisel SR, Ong JM, Kaul S, Cercek B, Rajavashisth TB, Sharifi B, Shah PK. Oxidized low-density lipoprotein regulates matrix metalloproteinase-9 and its tissue inhibitor in human monocyte-derived macrophages. Circulation.1999.99:993-998
34. Nicholls SJ, Cutri B, Worthley SG, Kee P, Rye KA, Bao S, Barter PJ.Impact of short-term administration of high-density lipoproteins and atorvastatin on atherosclerosis in rabbits.ArteriosclerThrombVascBiol.2005.25:2416-2421
35. Bellosta S, Gomaraschi M, Canavesi M, Rossoni G, Monetti M, Franceschini G, Calabresi L. Inhibition of mmp-2 activation and release as a novel mechanism for hdl-induced cardioprotection. FEBS letters.2006.580:5974-5978
36. Guidelines for the approach to the patient with severe hereditary alpha-1-antitrypsin deficiency. American thoracic society.Am Rev Respir Dis.1989.140:1494-1497
37. Bates SR, Tao JQ, Yu KJ, Borok Z, Crandall ED, Collins HL, Rothblat GH. Expression and biological activity of abca1 in alveolar epithelial cells.Am J Respir Cell MolBioil.2008.38:283-292
38. Sohrab S, Petrusca DN, Lockett AD, Schweitzer KS, Rush NI, Gu Y, Kamocki K, Garrison J, Petrache I. Mechanism of alpha-1 antitrypsin endocytosis by lung endothelium. FASEB J.2009.23:3149-3158
39. Petrache I, Fijalkowska I, Zhen L, Medler TR, Brown E, Cruz P, Choe KH, Taraseviciene-Stewart L, Scerbavicius R, Shapiro L, Zhang B, Song S, Hicklin D, Voelkel NF, Flotte T, Tuder RM. A novel antiapoptotic role for alpha1-antitrypsin in the prevention of pulmonary emphysema.Am J RespirCrit Care Med.2006.173:1222-1228
40. Petrache I, Fijalkowska I, Medler TR, Skirball J, Cruz P, Zhen L, Petrache HI, Flotte TR, Tuder RM. Alpha-1 antitrypsin inhibits caspase-3 activity, preventing lung endothelial cell apoptosis. Am J PAthol.2006.169:1155-1166
41. Lewis EC. Expanding the clinical indications for alpha-1-antitrypsin therapy.Mol Med 2012.18:957-70
42. Liu Z, Zhou X, Shapiro SD, Shipley JM, Twining SS, Diaz LA, Senior RM, Werb Z. The serpin alpha1-proteinase inhibitor is a critical substrate for gelatinase b/mmp-9 in vivo. Cell.2000.102:647-655
43. Toldo S, Seropian IM, Mezzaroma E, Van Tassell BW, Salloum FN, Lewis EC, Voelkel N, Dinarello CA, Abbate A. Alpha-1 antitrypsin inhibits caspase-1 and protects from acute myocardial ischemia-reperfusion injury. J Mol Cell Cardiol.2011.51:244-251
44. Blanco I, Lara B, de Serres F. Efficacy of alpha1-antitrypsin augmentation therapy in conditions other than pulmonary emphysema. Orphanet J Rare Dis.2011.6:14

45. Tran-Dinh A, Diallo D, Delbosc S, Varela-Perez LM, Dang QB, Lapergue B, Burillo E, Michel JB, Levoye A, Martin-Ventura JL, Meilhac O. HDL and endothelial protection. Br J Pharmacol. 2013. 169:493-511

46. Kimura T, Tomura H, Mogi C, Kuwabara A, Damirin A, Ishizuka T, Sekiguchi A, Ishiwara M, Im DS, Sato K, Murakami M, Okajima F.
Role of scavenger receptor class B type I and sphingosine 1-phosphate receptors in high density lipoprotein-induced inhibition of adhesion molecule expression in endothelial cells. J Biol Chem. 2006. 281:37457-67.

47. Nofer JR, Levkau B, Wolinska I, Junker R, Fobker M, von Eckardstein A, Seedorf U, Assmann G. Suppression of endothelial cell apoptosis by high density lipoproteins (HDL) and HDL-associated lysosphingolipids. J Biol Chem. 2001.276:34480-5.

48. Diab KJ, Adamowicz JJ, Kamocki K, Rush NI, Garrison J, Gu Y, Schweitzer KS,Skobeleva A, Rajashekhar G, Hubbard WC, Berdyshev EV, Petrache I.Stimulation of sphingosine 1-phosphate signaling as an alveolar cell survival strategy in emphysema. Am J Respir Crit Care Med. 2010. 181:344-52.

49. Mohanka M, Khemasuwan D, Stoller JK. A review of augmentation therapy for alpha-1 antitrypsin deficiency.Expert OpinBiolTher.2012.12:685-700

50. Tisi GM, Conrique A, Barrett-Connor E, Grundy SM.Increased high density lipoprotein cholesterol in obstructive pulmonary disease (predominant emphysematous type). Metabolism. 1981.30:340-6.

51. Reed RM, Iacono A, DeFilippis A, Eberlein M, Girgis RE, Jones S. Advanced chronic obstructive pulmonary disease is associated with high levels of high-density lipoprotein cholesterol. J Heart Lung Transplant. 2011.30:674-8.

52. Reed RM, Hashmi S, Eberlein M, Iacono A, Netzer G, DeFilippis A, Girgis RE, Toth PP, Scharf S, Jones S.Impact of lung transplantation on serum lipids in COPD. Respir Med. 201.105:1961-8.

53. Cirillo DJ, Agrawal Y, Cassano PA. Lipids and pulmonary function in the Third National Health and Nutrition Examination Survey. Am J Epidemiol. 2002.155:842-8.

54. Ubhi BK, Riley JH, Shaw PA, Lomas DA, Tal-Singer R, MacNee W, Griffin JL, Connor SC.Metabolic profiling detects biomarkers of protein degradation in COPD patients. Eur Respir J. 2012.40:345-55.

55. Björkerud S, Björkerud B. Lipoproteins are major and primary mitogens and growth promoters for human arterial smooth muscle cells and lung fibroblasts in vitro. Arterioscler Thromb. 1994.14:288-98.

FIGURE LEGENDS

Figure 1. High-density lipoprotein (HDL) enrichment with α1-antitrypsin (AAT) and study flow diagram. Western blot analysis for AAT and apolipoprotein A1 (ApoA1) before and after enrichment of HDL with AAT was performed, loading different amounts (in micrograms) of native HDL or HDL enriched in AAT (HDL-AAT) and commercially available purified AAT (A). Densitometric analysis showed that the concentration of AAT in HDL can be estimated at 0.2 μg/20 μg ApoA1 (10 μg AAT/mg apoA1). After HDL enrichment in AAT, the concentration of AAT in HDL particles rose to 50 μg AAT/mg apoA1. Antielastase activity of AAT (0.01–0.5 μg), native HDL, and HDL-AAT (1–20 μg), assayed using a chromogenic substrate for elastase, corroborate the results obtained by Western blot, showing a fivefold increase in antielastase activity after enrichment (B). Study flow diagram (C). Elastase-treated mice were divided into four groups injected, respectively, with saline, HDL (75 mg/kg body weight), HDL enriched in AAT (75 mg ApoA1–3.75 mgAAT/kg), or AAT alone (3.75 mg/kg). A control group consisting of sham-operated mice was also included in each set of experiment. Five groups of mice were used to assess alveolar destruction 3 weeks after the induction of emphysema (morphological study). In a second set of experiments, mice were killed at 6, 24, or 72 hours to determine different parameters in blood and in the bronchoalveolar lavage fluid (BALF). In a third set of experiments, mice (n = 4 per group) were imaged 6 hours after elastase instillation and 4 hours after injection with 1,1′-Dioctadecyl-3,3,3′,3′-tetramethylindodicarbocyanine-5,5′-disulfonic acid (DilC18)-labeled HDL, HDL-AAT, or saline.

Figure 2. HDL treatment reduced elastase-induced pulmonary emphysema. Representative hematoxylin and eosin staining on great-axis sagittal sections of the left lung (×100 original magnification) of sham mice with intratracheal instillation of saline (1), intratracheal elastase and intravenous injection of saline (2), intratracheal elastase and intravenous injection of HDL (3), intratracheal elastase and intravenous injection of HDL-AAT (4), and intratracheal elastase and intravenous injection of AAT alone (5). Mice were killed at Day 28. The diagram represents the mean chord length of alveoli. Data are means (± SD); *$P < 0.05$ versus group 1, †$P < 0.05$ versus groups 2 and 3, #$P < 0.05$ versus group 4. ΔE, mean increase in chord length (μm) due to elastase instillation.

Figure 3. HDLs accumulate in the lung of emphysematous mice. (A) Fluorescence molecular imaging of DilC18-labeled HDL bioavailability to the lung in vivo and ex vivo (n = 4 per group). Mice were instilled with saline/elastase, injected with DilC18-HDL at 2 hours, and then imaged, using the IVIS Imaging System, at 6 hours. After mice were killed, the whole cardiopulmonary block was extracted for a more precise determination of lung signal by ex vivo fluorescence imaging (lower panel). (B) Immunohistofluorescence staining showing the binding of exogenous DilC18-HDL and DilC18-HDL-AAT (red) to the lung from emphysematous or control mice. Nuclei were stained by 4′,6-diamidino-2-phenylindole (DAPI; blue). We incubated labeled HDL and HDL-AAT for 2 hours at 37°C on slides containing lungs from mice instilled with elastase or saline. (C) Affinity of HDL and HDL-AAT for elastase. HDL binding to elastase was assessed with increasing concentrations of DilC18-HDL (closed circles) or DilC18-HDL-AAT (open circles). Data were analyzed using a nonlinear regression equation applied to a single binding site model. Results (means ± SEM) are from three independent experiments performed in duplicate or triplicate.*$P < 0.05$ versus HDL-elastase and HDL-AAT-saline.

Figure 4. AAT vectorization by HDL. Mice were instilled with saline/elastase and then injected (at 2 h) with HDL (75 mg/kg), HDL-AAT (75 mg/kg ApoA1–3.75 mg/ml AAT), or AAT alone (3.75 mg/kg). At 6 hours later, the mice were killed, perfused with saline, and the lungs were removed for detection of exogenous human ApoA1 and AAT by Western blot and immunofluorescence. (A) Western blot analysis and semiquantitative assessment (right) of ApoA1 and AAT from lung extracts (50 μg of total protein). (B) Double immunohistofluorescence staining and semiquantitative assessment (right) showing the presence of exogenous ApoA1 (green) and AAT (red) in the lung. Nuclei were stained by DAPI (blue). (C) Cellular ApoA1 and AAT colocalization in the lung of an HDL-AAT–injected mouse. GADPH, glyceraldehyde 3-phosphate dehydrogenase. *$P < 0.05$ versus the same group treated with saline. †$P < 0.05$ versus mice injected with nonenriched HDL or AAT alone.

Figure 5. HDL treatment decreased elastase-induced pulmonary inflammation. (A) Neutrophil and (C) macrophage concentrations in the BALF of: (1) control mice (intratracheal injection of saline); (2) mice treated by intratracheal elastase and intravenous injection of saline; (3) intratracheal elastase and intravenous injection of

HDL; (4) intratracheal elastase and intravenous injection of HDL-AAT; and (5) intratracheal elastase and intravenous injection of AAT. Data are means (± SD). All groups were significantly different from group 1 ($P < 0.05$) unless otherwise stated *. †$P < 0.05$ versus group 2, #$P < 0.05$ versus group 4. *Not significantly different from group 1 ($P > 0.05$). Immunohistochemistry showing lung infiltration of neutrophils (B) and macrophages (D) 6 hours after instillation with elastase/saline and treated with saline, HDL, HDL-AAT, or AAT alone. Naive IgGs, control section treated with the same amount of nonimmune IgGs as used for specific immunostaining.

Figure 6. HDL treatment prevented elastase-induced production of inflammatory cytokines. Cytometric Bead Array Mouse Inflammation Kit was used on BALF (A) and plasma (B) to quantify IL-6, monocyte chemoattractant protein (MCP)-1, and TNF-α protein levels in: (1) sham mice; (2) mice that underwent intratracheal elastase instillation and intravenous saline injection; (3) intratracheal elastase plus intravenous HDL; (4) intratracheal elastase plus intravenous HDL-AAT; (5) and intratracheal elastase plus intravenous AAT. Data are means (± SD); *$P < 0.05$ versus group 1, †$P < 0.05$ versus group 2 and 3.

Figure 7. HDL treatment reduced neutrophil elastase and matrix metalloproteinase (MMP)-2/-9 activities in emphysematous lung. Representative gelatinzymography of BALF (A) at the 6th, 24th, and 72nd hours in sham mice (lane 1), mice with intratracheal elastase instillation and intravenous injection of saline (lane 2), intratracheal elastase plus intravenous HDL (lane 3), intratracheal elastase plus intravenous HDL-AAT (lane 4), and intratracheal elastase plus intravenous AAT (lane 5). Densitometric quantification of elastase (B), MMP-9 (C), and MMP-2 (D) gelatinolytic activities in BALF. Elastase activity was not detected in BALF at 72 hours in any group. Data are means (± SD); *$P < 0.05$ versus group 1, †$P < 0.05$ versus groups 2 and 3.

Figure 8. HDL-AAT treatment decreased fibronectin degradation in emphysematous lung. Representative Western blots showing fibronectin degradation products at the 24th and 72nd hours. (1) Sham mice; (2) intratracheal elastase plus intravenous saline; (3) intratracheal elastase plus intravenous HDL; (4) intratracheal elastase plus intravenous HDL-AAT; and (5) intratracheal elastase plus intravenous AAT. No fibronectin degradation was detected in BALF at 6 hours in any group. Densitometry quantification

of fibronectin fragments (diagram). Data are means (± SD); *P < 0.05 versus group 1, †P < 0.05 versus groups 2 and 3.

Figure 1

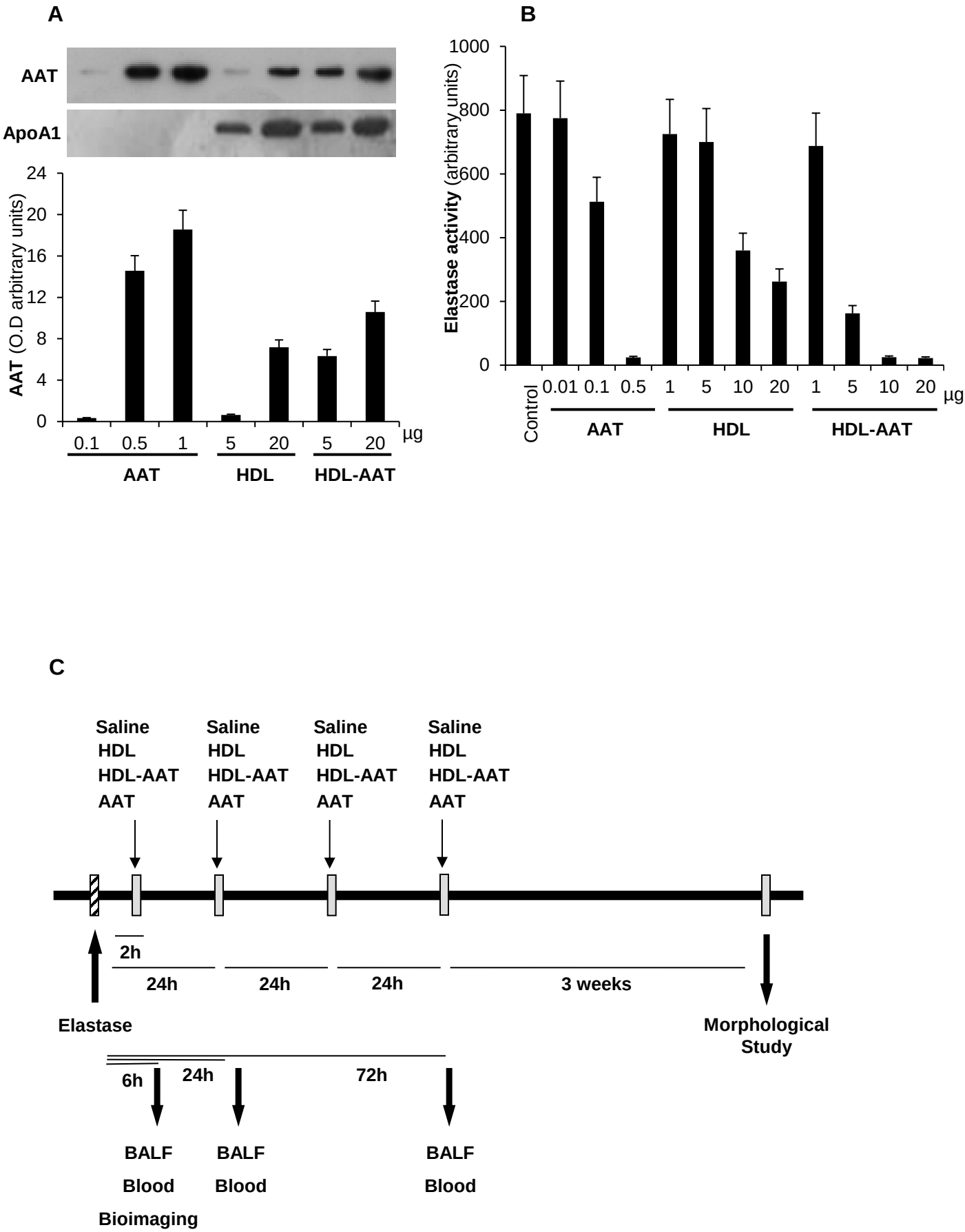
A
AAT
ApoA1
AAT (O.D arbitrary units)
24
20
16
12
8
4
0
0.1
0.5
1
5
20
5
20
µg
AAT
HDL
HDL-AAT
B
Elastase activity (arbitrary units)
1000
800
600
400
200
0
Control
0.01
0.1
0.5
1
5
10
20
1
5
10
20
µg
AAT
HDL
HDL-AAT
C
Saline
HDL
HDL-AAT
AAT
Saline
HDL
HDL-AAT
AAT
Saline
HDL
HDL-AAT
AAT
Saline
HDL
HDL-AAT
AAT
2h
24h
24h
24h
3 weeks
Elastase
Morphological Study
6h
24h
72h
BALF
Blood
Bioimaging
BALF
Blood
BALF
Blood

Figure 2

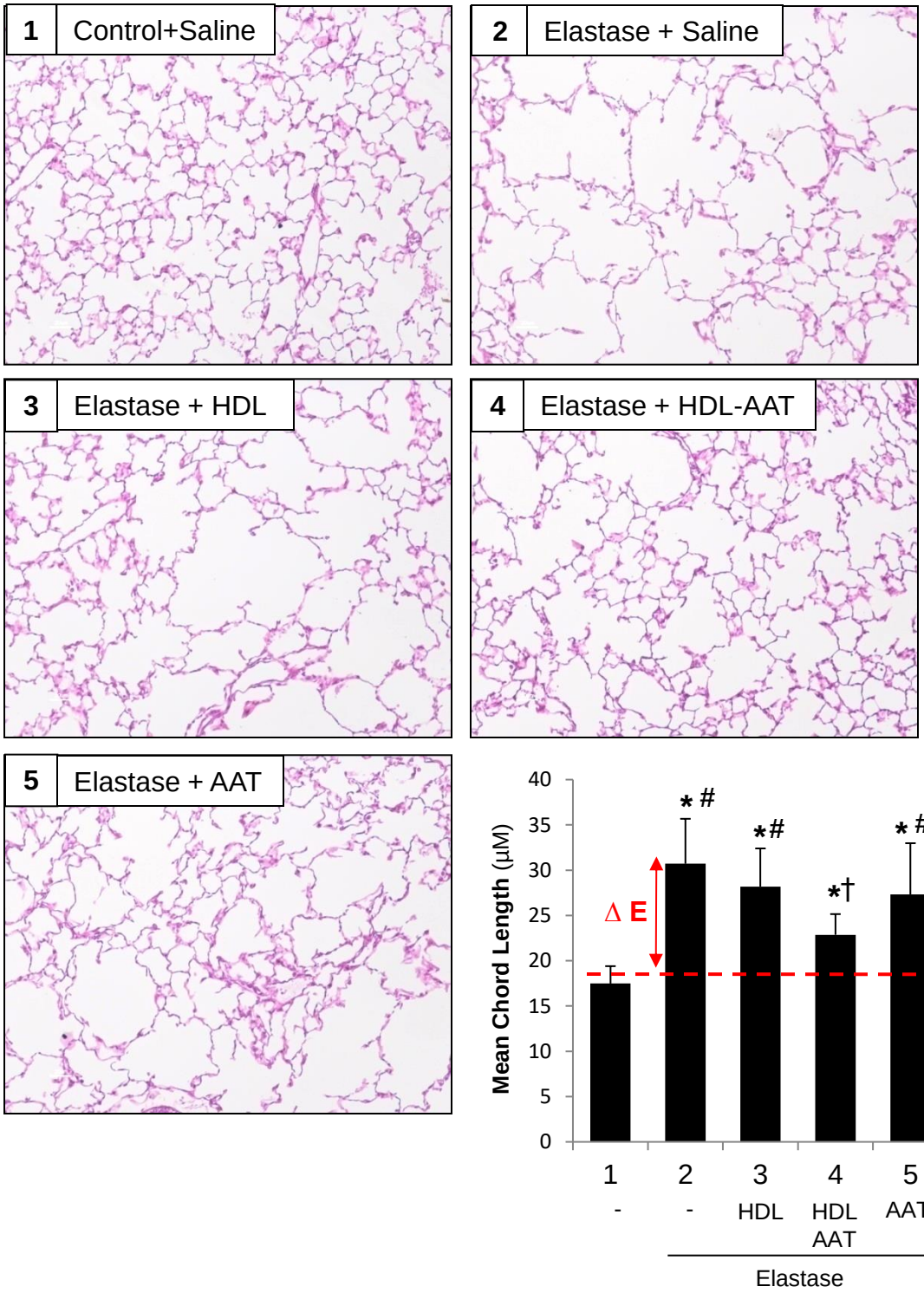
1 Control+Saline
2 Elastase + Saline
3 Elastase + HDL
4 Elastase + HDL-AAT
5 Elastase + AAT
Mean Chord Length (μM)
40
35
30
25
20
15
10
5
0
ΔE
*#
*#
*†
*#
1
-
2
-
3
HDL
4
HDL
AAT
5
AAT
Elastase

Figure 3

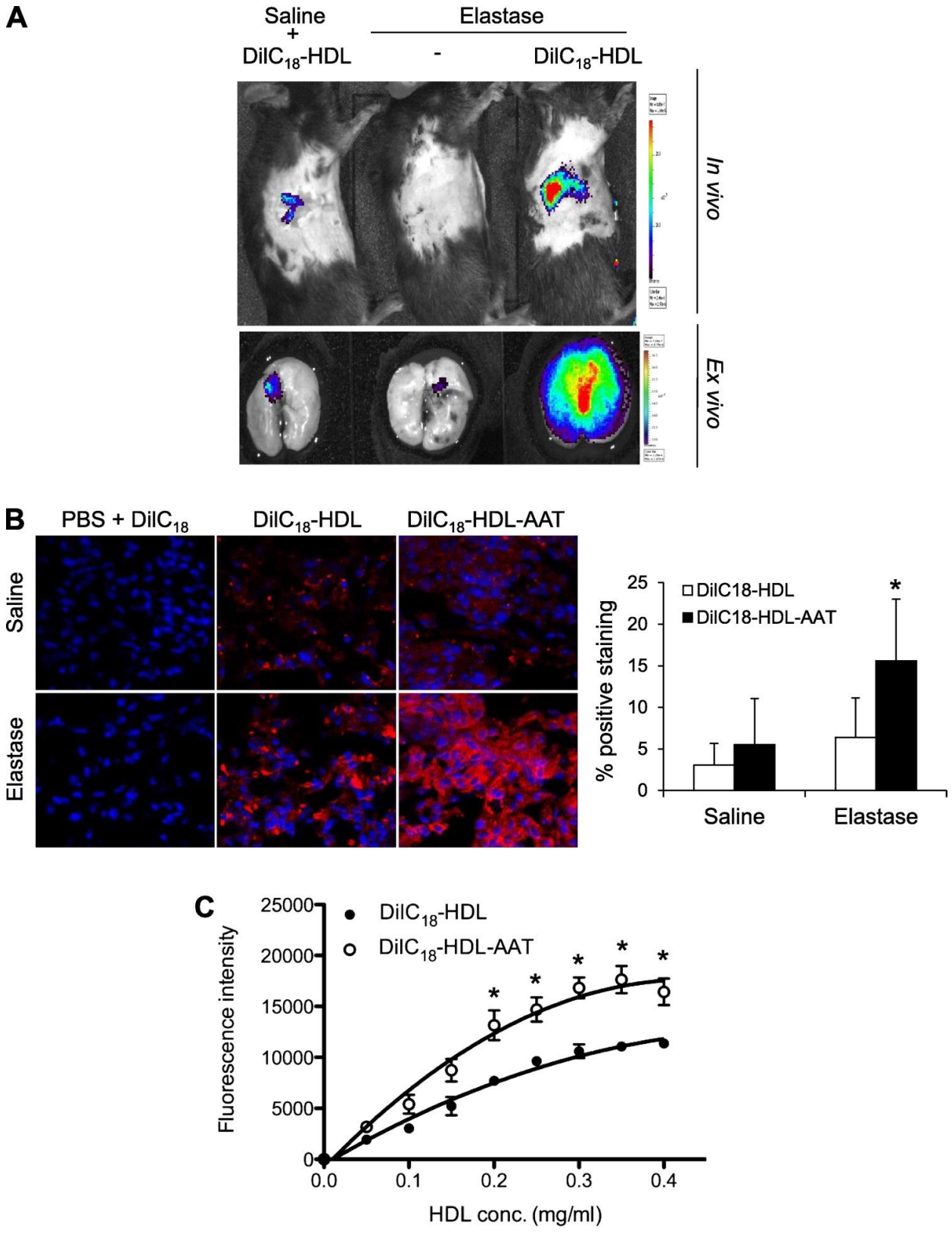
A
Saline + DiIC18-HDL
Elastase
-
DiIC18-HDL
In vivo
Ex vivo
B
PBS + DiIC18
DiIC18-HDL
DiIC18-HDL-AAT
Saline
Elastase
% positive staining
DiIC18-HDL
DiIC18-HDL-AAT
Saline
Elastase
C
Fluorescence intensity
DiIC18-HDL
DiIC18-HDL-AAT
HDL conc. (mg/ml)

Figure 4

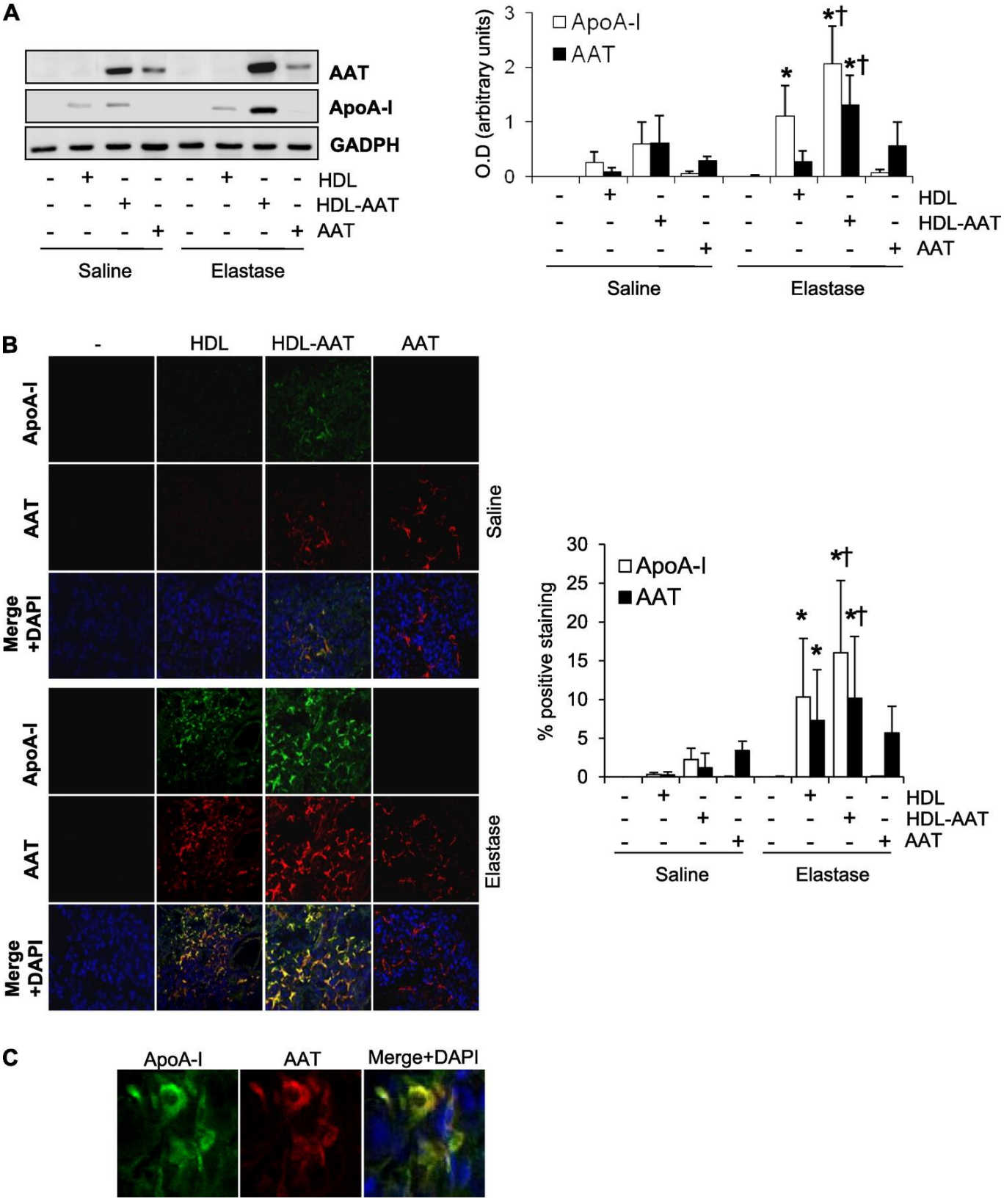
A
AAT
ApoA-I
GADPH
HDL
HDL-AAT
AAT
Saline
Elastase
O.D (arbitrary units)
ApoA-I
AAT
B
HDL
HDL-AAT
AAT
ApoA-I
AAT
Merge +DAPI
Saline
Elastase
% positive staining
C
ApoA-I
AAT
Merge+DAPI

Figure 5

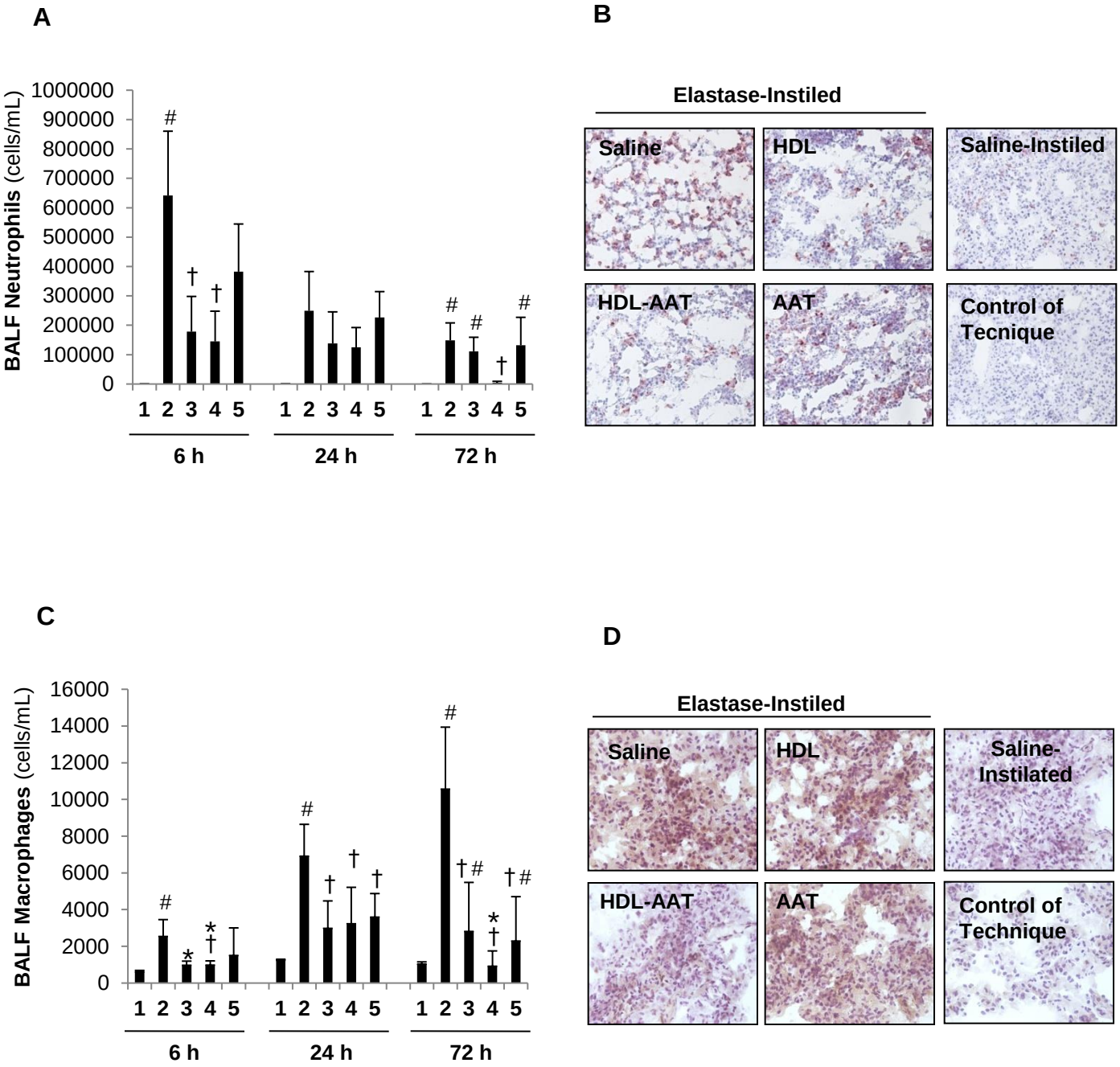
A
B
C
D
BALF Neutrophils (cells/mL)
1000000
900000
800000
700000
600000
500000
400000
300000
200000
100000
0
1 2 3 4 5 1 2 3 4 5 1 2 3 4 5
6 h
24 h
72 h
Elastase-Instiled
Saline
HDL
Saline-Instiled
HDL-AAT
AAT
Control of Tecnique
BALF Macrophages (cells/mL)
16000
14000
12000
10000
8000
6000
4000
2000
0
Saline-Instilated
Control of Technique

Figure 6

A: BALF

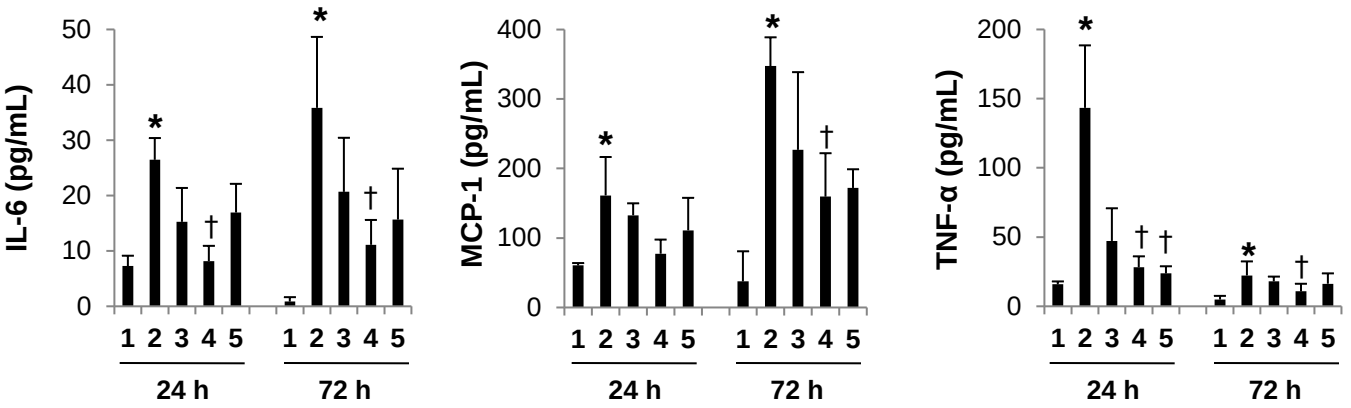

B: Plasma

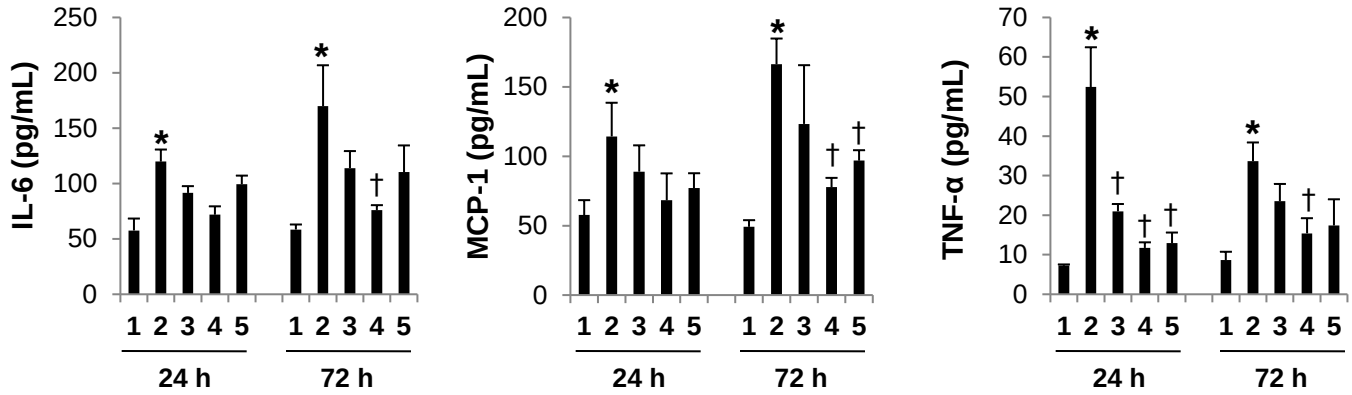

Figure 7

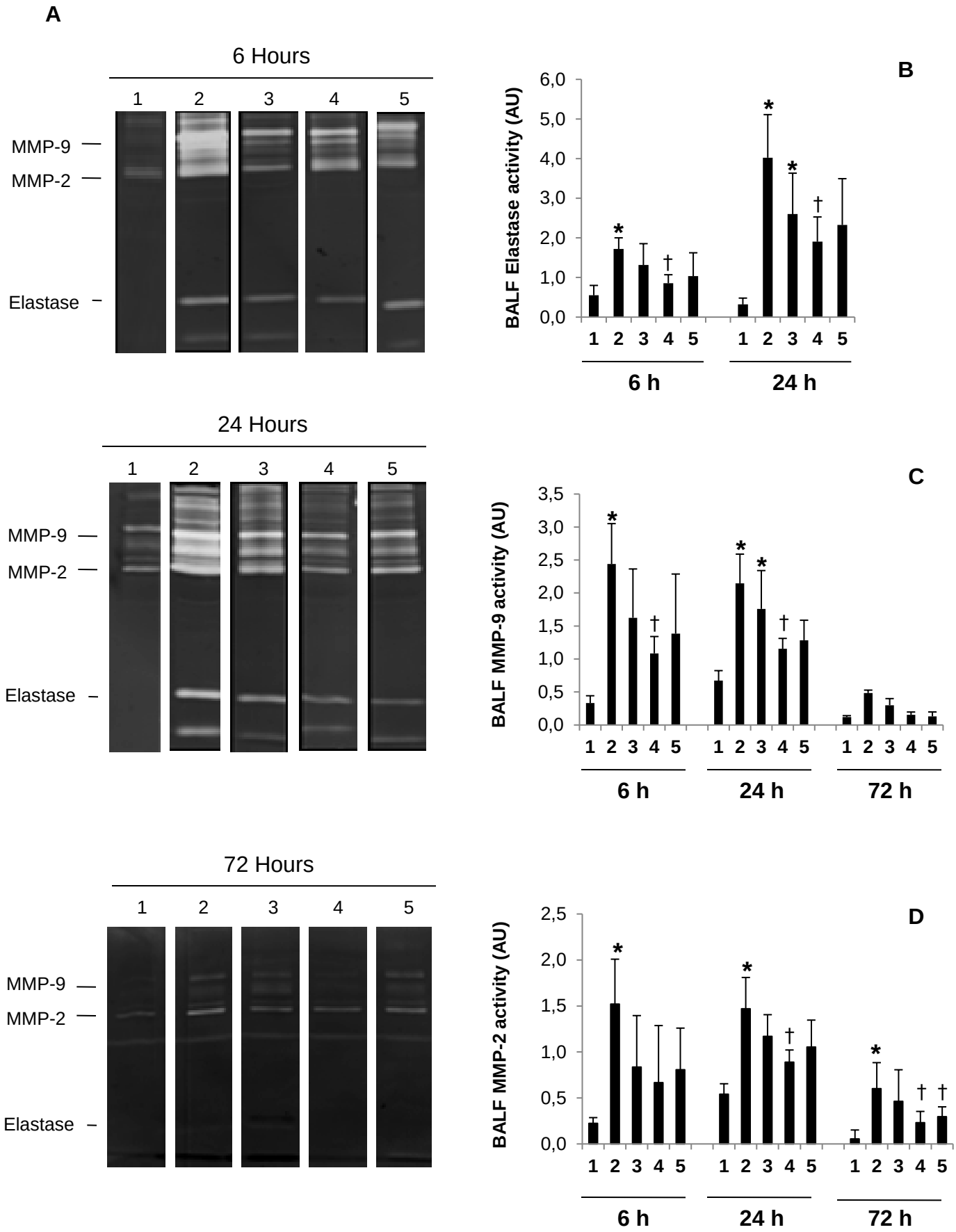
A
6 Hours
1 2 3 4 5
MMP-9
MMP-2
Elastase
24 Hours
1 2 3 4 5
MMP-9
MMP-2
Elastase
72 Hours
1 2 3 4 5
MMP-9
MMP-2
Elastase
B
BALF Elastase activity (AU)
6,0
5,0
4,0
3,0
2,0
1,0
0,0
1 2 3 4 5 1 2 3 4 5
6 h
24 h
C
BALF MMP-9 activity (AU)
3,5
3,0
2,5
2,0
1,5
1,0
0,5
0,0
1 2 3 4 5 1 2 3 4 5 1 2 3 4 5
6 h
24 h
72 h
D
BALF MMP-2 activity (AU)
2,5
2,0
1,5
1,0
0,5
0,0
1 2 3 4 5 1 2 3 4 5 1 2 3 4 5
6 h
24 h
72 h

Figure 8

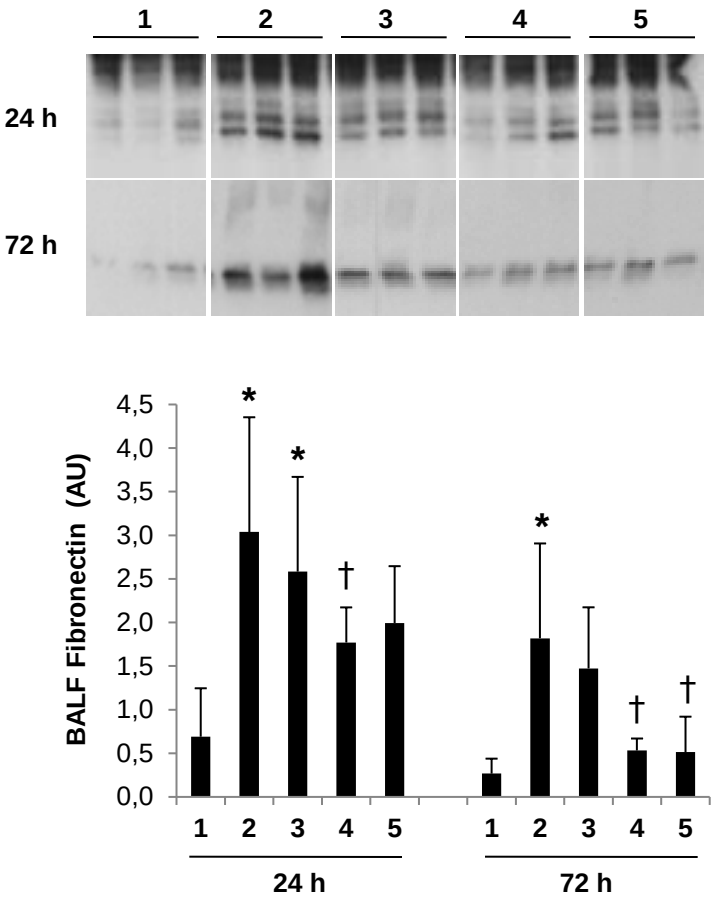
1
2
3
4
5
24 h
72 h
BALF Fibronectin (AU)
4,5
4,0
3,5
3,0
2,5
2,0
1,5
1,0
0,5
0,0
*
*
†
*
†
†
1 2 3 4 5
1 2 3 4 5
24 h
72 h

Online Data Supplement

Title: High Density Lipoproteins potentiate alpha-1 antitrypsin therapy in elastase-induced pulmonary emphysema

Authors: Juan-Antonio Moreno, Almudena Ortega-Gomez, Alfonso Rubio-Navarro, Liliane Louedec, Benoit Ho-Tin-Noé, Giuseppina Caligiuri, Antonino Nicoletti, Angelique Levoye, Laurent Plantier, and Olivier Meilhac

Figure E1. Inhibition of mouse neutrophil elastase by human purified AAT. Neutrophil elastase activity in lysates from C57/BL6 mouse bone marrow cells was measured in the presence of increasing concentrations of human AAT. Results are expressed as a percentage (mean ± SD, n = 3) relative to the activity measured in the absence of AAT. Data were fitted to a hyperbolic decay equation allowing calculation of the AAT concentration that produced 50 % of the inhibitory effect (EC50 = 158 µg/mL). The concentration of neutrophil elastase in lysates from C57BL/6 mouse bone marrow cells was of 12 µg/mL.Each plot is representative of 3 independent experiments showing comparable results.

Figure E2. HDL-AAT treatment reduced elastase-induced pulmonary emphysema. The diagram represents the mean chord length of alveoli of sham mice with intra-tracheal instillation of saline, intra-tracheal elastase and i.v. injection of saline, intra-tracheal elastase and i.v. injection of LDL, intra-tracheal elastase and i.v. injection of AAT alone, intra-tracheal elastase and i.v. injection of HDL, intra-tracheal elastase and i.v. injection of HDL and AAT simultaneusly, and intra-tracheal elastase and i.v. injection of HDL-AAT. Mice of the HDL-AAT group were injected with HDL that were incubated for 16 hours with AAT at 37°C to obtain HDL enriched in AAT, whereas mice of the HDL/AAT group received a simultaneous injection of HDL and AAT. Mice were euthanized at day 28. Data are means ± SD, * $P < 0.05$ vs sham group, # $P < 0.05$ vs group instilated with elastase and injected with saline. ΔE represents the mean increase in chord length (µm) due to elastase instillation.

Figure E3. X-ray and fluorescence molecular imaging of DilC18-labelled HDL bio-availability to the lung in vivo. To colocalize lung position with lung fluorescence signal, mice were injected with DilC18-HDL and 4 hours later imaged using the IVIS Imaging System. X-ray image was acquired using the ultrafast Lunar PIXImus Densitometer (GE Medical Systms, Salt Lake City, UT) in a representative live animal after fluorescence imaging analysis.

Figure E4. ABCA1 and SRB-1 expression in elastase-induced pulmonary emphysema. Mice were instilled with saline/elastase and then lung were extracted from 0 to 48h (n=4 per group). ABCA1 and SRB-1 mRNA expression was determined by quantitative RT-PCR in lung tissue homogenate.

Figure E5. Fluorescence molecular imaging of DilC18-labelled HDL bio-availability to the lung ex vivo. Mice were subjected to saline or elastase instillation, injected with DilC18-HDL or DilC18-HDL-AAT at H2 and then the whole cardiopulmonary block was extracted and 6 hours later imaged using the IVIS Imaging System.

Figure E6. HDL treatment decreased cigarette-induced pulmonary inflammation. Neutrophil (A), and macrophage (B) concentrations in the bronchoalveolar lavage fluid (BALF) of control mice (non-smoke exposed mice), smoke-exposed mice and i.v saline, smoke-exposed mice and i.v HDL, smoke-exposed mice and i.v HDL-AAT, and smoke-exposed mice and i.v AAT. (C) IL-6, (D) MCP-1 and (E) TNF-α mRNA expression in lung tissue homogenate from cigarette smoke-exposed mice. Data are means ± SD. * $P<0.05$ vs control group. † $P<0.05$ vs smoke-exposed mice and i.v saline.

Figure E1

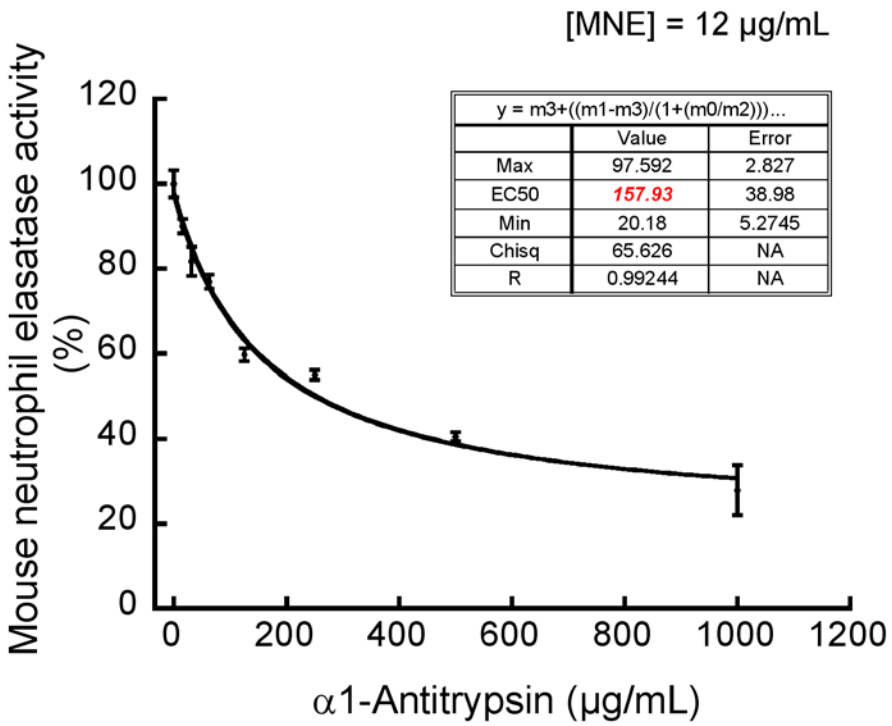

Figure E1. Inhibition of mouse neutrophil elastase by human purified AAT. Neutrophil elastase activity in lysates from C57/BL6 mouse bone marrow cells was measured in the presence of increasing concentrations of human AAT. Results are expressed as a percentage (mean ± SD, n = 3) relative to the activity measured in the absence of AAT**.** Data were fitted to a hyperbolic decay equation allowing calculation of the AAT concentration that produced 50 % of the inhibitory effect (EC50 = 158 µg/mL). The concentration of neutrophil elastase in lysates from C57/BL6 mouse bone marrow cells was of 12 µg/mL. Each plot is representative of 3 independent experiments showing comparable results.

Figure E2

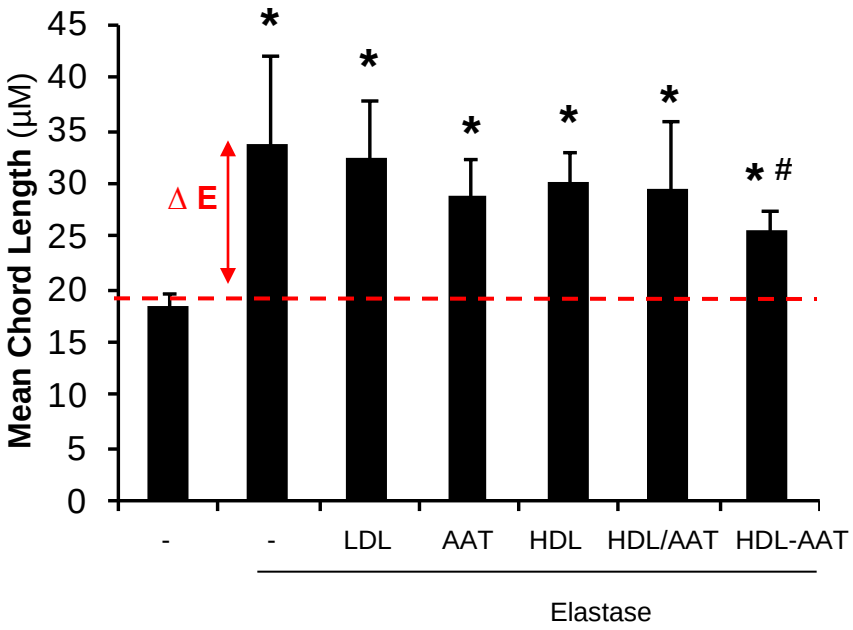

Figure E2. HDL+AAT treatment reduced elastase-induced pulmonary emphysema. The diagram represents the mean chord length of alveoli of sham mice with intra-tracheal instillation of saline, intra-tracheal elastase and i.v. injection of saline, intra-tracheal elastase and i.v. injection of LDL, intra-tracheal elastase and i.v. injection of AAT alone, intra-tracheal elastase and i.v. injection of HDL, intra-tracheal elastase and i.v. injection of HDL and AAT simultaneusly, and intra-tracheal elastase and i.v. injection of HDL+AAT. Mice of the HDL-AAT group were injected with HDL that were incubated for 16 hours with AAT at 37° C to obtain HDL enriched in AAT, whereas mice of the HDL/AAT group received a simultaneous injection of HDL and AAT. Mice were euthanized at day 28. Data are means ± SD, * $P < 0.05$ vs sham group, # $P < 0.05$ vs group instilated with elastase and injected with saline. ΔE represents the mean increase in chord length (µm) due to elastase instillation.

Figure E3

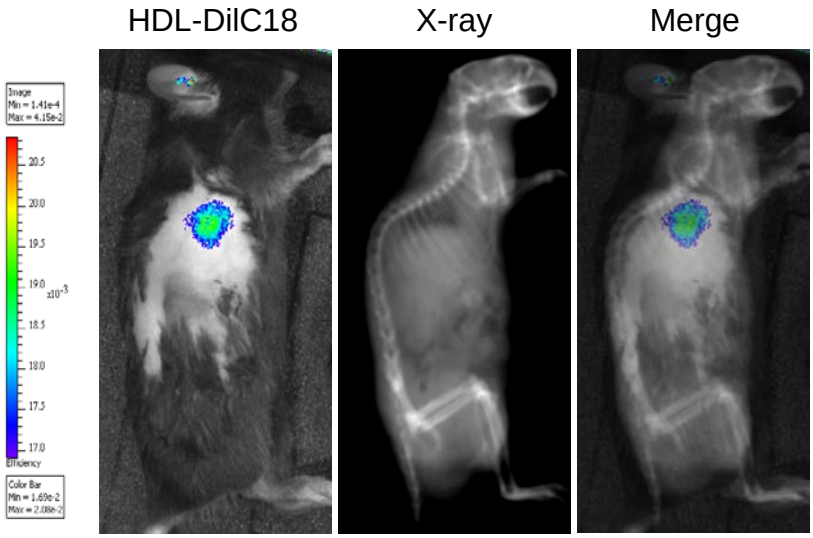

Figure E3. X-ray and fluorescence molecular imaging of DilC18-labelled HDL bio-availability to the lung in vivo. To colocalize lung position with lung fluorescence signal, mice were injected with DilC18-HDL and 4 hours later imaged using the IVIS Imaging System. X-ray image was acquired using the ultrafast Lunar PIXImus Densitometer (GE Medical Systms, Salt Lake City, UT) in a representative live animal after fluorescence imaging analysis.

Figure E4

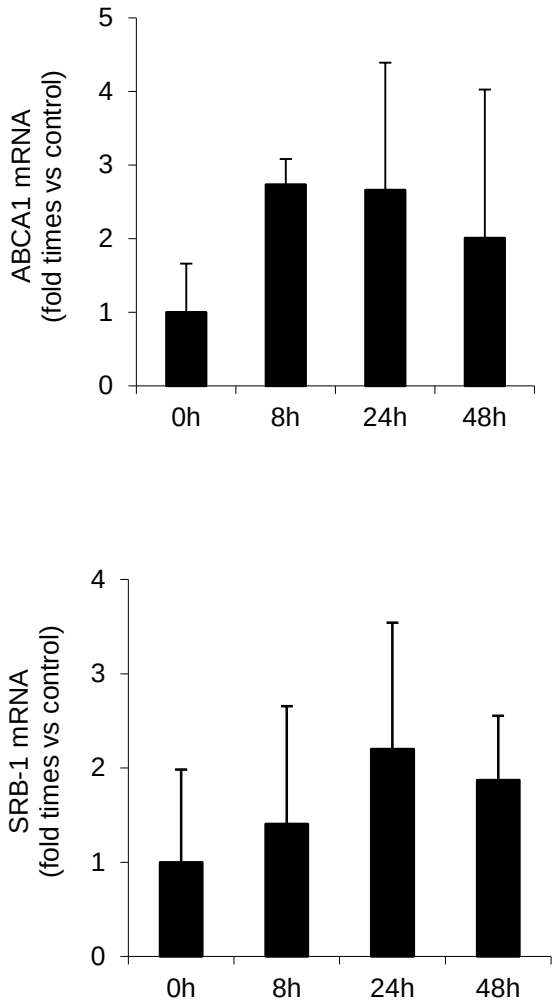
ABCA1 mRNA
(fold times vs control)
5
4
3
2
1
0
0h
8h
24h
48h
SRB-1 mRNA
(fold times vs control)
4
3
2
1
0
0h
8h
24h
48h

Figure E5

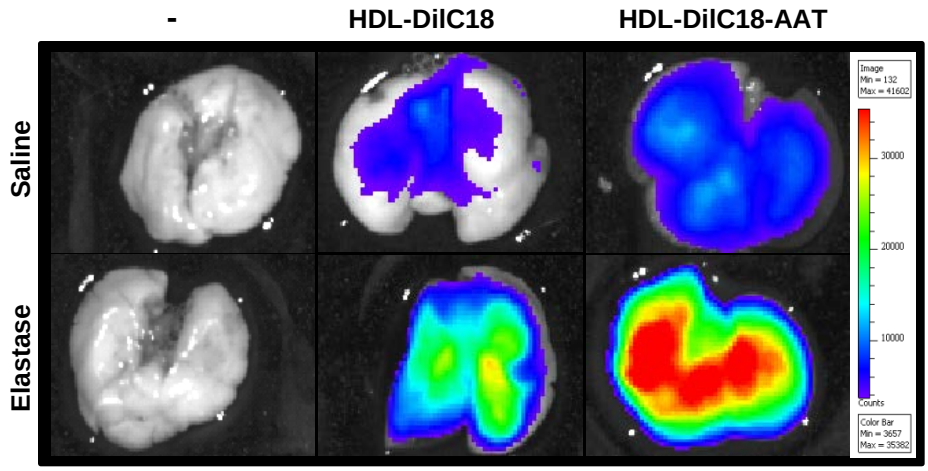

Figure E5. Fluorescence molecular imaging of DilC18-labelled HDL bio-availability to the lung ex vivo. Mice were subjected to saline or elastase instillation, injected with DilC18-HDL or DilC18-HDL-AAT at H2 and then the whole cardiopulmonary block was extracted and 6 hours later imaged using the IVIS Imaging System.

Figure E6

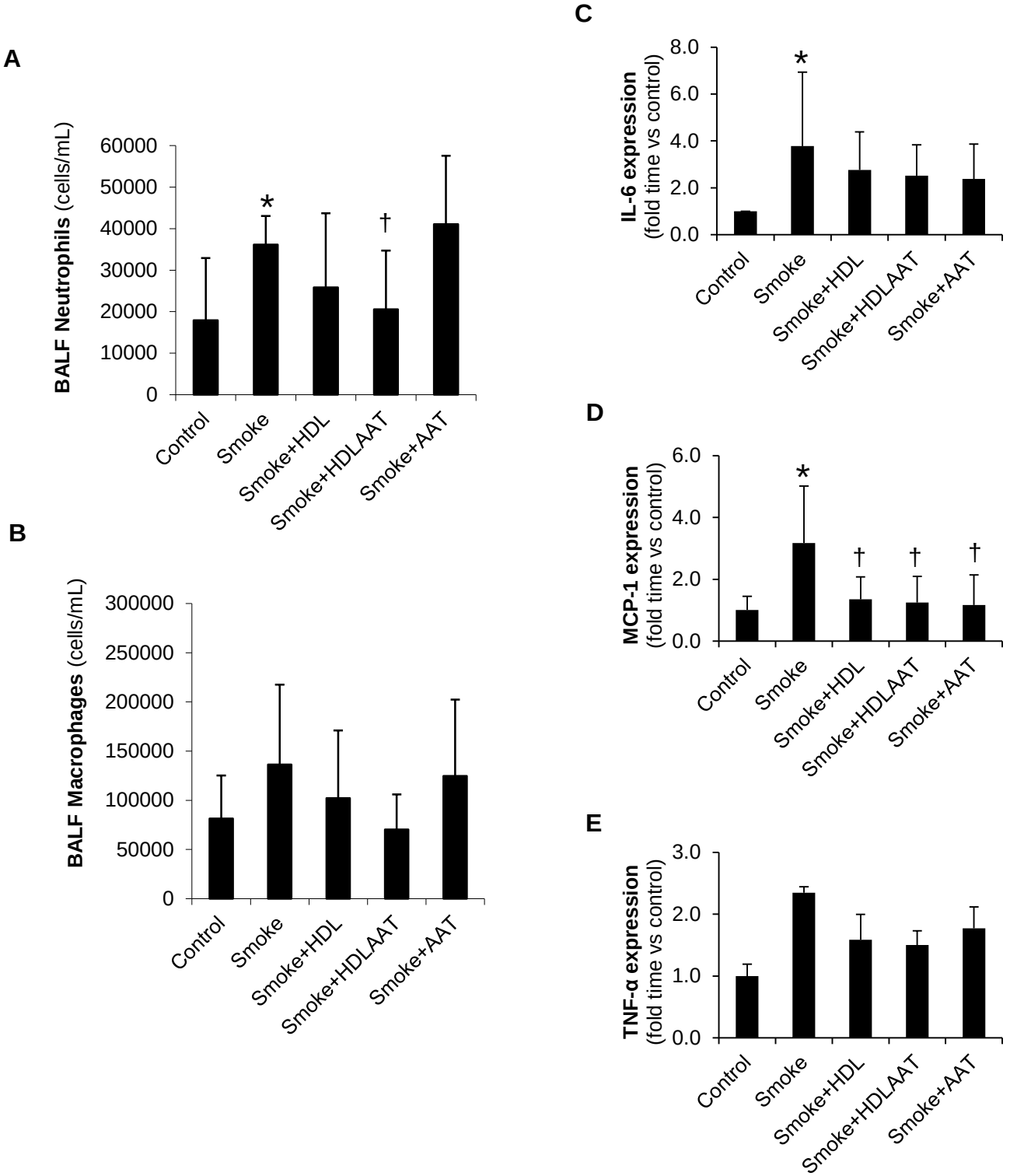
A
BALF Neutrophils (cells/mL)
60000
50000
40000
30000
20000
10000
0
*
†
Control
Smoke
Smoke+HDL
Smoke+HDLAAT
Smoke+AAT
B
BALF Macrophages (cells/mL)
300000
250000
200000
150000
100000
50000
0
Control
Smoke
Smoke+HDL
Smoke+HDLAAT
Smoke+AAT
C
IL-6 expression
(fold time vs control)
8.0
6.0
4.0
2.0
0.0
*
Control
Smoke
Smoke+HDL
Smoke+HDLAAT
Smoke+AAT
D
MCP-1 expression
(fold time vs control)
6.0
4.0
2.0
0.0
*
†
†
†
Control
Smoke
Smoke+HDL
Smoke+HDLAAT
Smoke+AAT
E
TNF-α expression
(fold time vs control)
3.0
2.0
1.0
0.0
Control
Smoke
Smoke+HDL
Smoke+HDLAAT
Smoke+AAT